THE THERAPEUTIC POTENTIAL OF GAMMA-BURST OSCILLATIONS (GBOS) DELIVERED BY LOW-FIELD MAGNETIC STIMULATION (LFMS) IN A RODENT MODEL OF FOCAL CORTICAL ISCHEMIC STROKE.

A Thesis Submitted to the
College of Graduate and Postdoctoral Studies
In Partial Fulfillment of the Requirements
For the Degree of Master of Science
In the Department of Anatomy, Physiology & Pharmacology
University of Saskatchewan
Saskatoon

By

HYE JI KIM

Permission to Use

In presenting this thesis in partial fulfillment of the requirements for a postgraduate degree from the University of Saskatchewan, I agree that the Libraries of this University may make it freely available for inspection. I further agree that permission for copying of this thesis in any manner, in whole or in part, for scholarly purposes may be granted by the professor or professors who supervised my thesis work or, in their absence, by the Head of the Department or the Dean of the College in which my thesis was done. It is understood that any copy or publication or use of this thesis or parts thereof for financial gain shall not be allowed without my written permission. It is also understood that due recognition shall be given to me and to the University of Saskatchewan in any scholarly use which may be made of any material in my thesis.

Requests for permission to copy or make other uses of materials in this thesis in whole or part should be addressed to:

Head of the Department of Anatomy, Physiology & Pharmacology
2D01 Health Science Building
107 Wiggins Road
Saskatoon, Saskatchewan
Canada S7N 5E5

OR

Dean of the College of Graduate and Postdoctoral Studies
116 Thorvaldsen Building
110 Science Place
Saskatoon, Saskatchewan
Canada S7N 5C9

Abstract

Many stroke survivors are affected by emotional and cognitive impairments that are difficult to treat. The current study uses a focal cortical ischemic stroke model called pial vessel disruption (PVD), which results in a non-reperfusion lesion in the right hemisphere. Previous studies have shown that PVD increases adenosine signalling, leading to the persistent stimulation and subsequent internalization of the adenosine A1 receptor (A1R), as well as the compensatory upregulation of the adenosine A2 receptor (A2AR) in the hippocampus. This adenosine receptor remodeling decreases cell surface expressions of the α-amino-3-hydroxy-5-methyl-4-isoxazolepropionic acid (AMPA) glutamate receptor subunits GluA1 and GluA2, thereby impairing hippocampal long-term potentiation (LTP). Moreover, cognitive deficits along with depression- and anxiety-like behaviours are demonstrated by rats following PVD. To better understand how neural oscillations affect post-PVD cell signalling and behaviour, LFMS delivering GBOs (40 Hz) was applied once-daily for three days following PVD. The literature suggests that ischemic stroke desynchronizes hippocampal gamma oscillations (30-80 Hz). This range of neural frequencies underlie higher cognitive processes such as learning and memory. Hippocampal-dependent cognition is crucial for encoding healthy emotional memories. Thus, LFMS may be normalizing adenosine signalling and resynchronizing endogenous gamma oscillations to have an overall therapeutic effect on post-PVD behavioural changes. Indeed, three LFMS treatments improved various aspects of depression- and anxiety-like behaviours, as well as hippocampal-dependent spatial memory in rats that underwent PVD. Moreover, LFMS equalized LTP between the ipsilateral and contralateral hippocampi and protected both hemispheric regions from cell death and neurodegeneration. Based on these results, LFMS may have a neuroprotective effect through either decreasing extracellular adenosine concentrations, preventing persistent A1R stimulation, or decreasing the compensatory upregulation of A2AR in the hippocampus following PVD.

Acknowledgements

This thesis would not have been possible without the immense support I received from the following people. First and foremost, I would like to thank Dr. Francisco Cayabyab, who took a chance on me and thoroughly believed in my passion for neuroscience. Aside from the numerous technical skills I acquired throughout this degree, Dr. Cayabyab's mentorship empowered me to think creatively and pursue my independent scientific thought processes. This provided me with self-confidence and motivation as a young woman in STEM.

I would also like to thank my graduate advisory committee members Dr. Stan Bardal, Dr. Changiz Taghibiglou, and Dr. Yanbo Zhang. The valuable lessons I learned from each unique member allowed me to conduct my research in a well-rounded and insightful manner. Dr. Taghibiglou and Dr. Zhang provided expertise in areas that I had little access to on my own. Dr. Bardal's equipoise and informational support helped me to stay focused on my goals.

I am extremely grateful for all of my lab colleagues, especially Michael Zaki, Adelaide Amah, Jasleen Saini, Jocelyn Stockwell, and Elisabet Jakova. These individuals taught me everything I know in the lab. I appreciate their tremendous help in my lab work, all of our late nights spent experimenting together, and every heart-felt conversation we had about our futures.

Finally, I would like to thank my parents, Hyemi, David, and the Kisby-Petrishen-Ha family. Their unconditional love and support constantly reminded me of my purpose in this world. I was either a high-velocity stress ball or a grumpy troll for 16 straight months. They always saw through the difficult times, and they are my entire heart.

The majority of my degree was generously funded by Dr. Cayabyab, as well as the University of Saskatchewan College of Medicine.

Table of Contents

List of Figures

Chapter 1: Introduction

1.1 Ischemic Stroke

1.1 Introduction to Ischemic Stroke

Stroke is one of the leading causes of death and disability worldwide (Johnson, Onuma, Owolabi, & Sachdev, 2016). Ischemic strokes are characterized by the occlusion of a brain arterial blood vessel due to a thrombus or embolus (Durukan & Tatlisumak, 2007). This leads to a deprivation of oxygen and nutrients to brain tissue. Although ischemic strokes account for 85-87% of all strokes, immediate treatment and diligent rehabilitation can save lives and effectively rescue functions (Bansal, Sangha, & Khatri, 2013). Depending on the size, location, and duration of vessel disruption, tissue plasminogen activator can lyse the clot and restore blood flow. In some cases, vessel disruption does not result in reperfusion and the ischemic lesion becomes permanent (Bansal et al., 2013). Regardless of its duration, ischemia can initiate downstream neurodegenerative signalling that affects the immediate injury site as well as other vulnerable brain regions such as the hippocampus. These disruptions give rise to mood disorders such as post-stroke depression (PSD) and post-stroke anxiety (PSA), as well as cognitive impairments. Rehabilitation may proceed over weeks to years, and commonly consist of pharmacotherapy, psychotherapy, and physiotherapy (NIH, 2018). Neuromodulatory therapies such as repetitive transcranial magnetic stimulation (rTMS) may also be effective by targeting downstream neurodegeneration from an electrophysiological standpoint (Al-Harbi & Qureshi, 2012; Tyler et al., 2008).

1.1.2 Hippocampal Vulnerability in Ischemic Stroke

The hippocampus is particularly vulnerable to ischemia (Schmidt-Kastner & Freund, 1991). This could partly be due to its greatly elaborated vasculature supplying the Sommer's sector

of the CA1, and its location between the carotid and vertebrobasilar arteries (Tatu & Vuillier, 2014). In a study where monkey brains underwent 20 minutes of global ischemia followed by reperfusion, the motor cortex was significantly resistant to downstream neurodegeneration compared to the hippocampus (Zhu et al., 2012). Damage to the CA1 pyramidal neurons are of particular interest when it comes to ischemic stroke. In one study, transient focal ischemia selectively damaged the CA1 pyramidal neurons leaving the neurons of the CA3 and dentate gyrus intact (Harry & Lefebvre d'Hellencourt, 2003). Moreover, the loss of CA1 pyramidal neurons due to an ischemic stroke correlated with spatial memory deficits that were not observed after damage to the CA3 and dentate gyrus (Volpe, Davis, Towle, & Dunlap, 1992). As the hippocampus is responsible for a large spectrum of behaviours, ischemic damage to its neuronal populations may result in significant neurological and psychiatric symptoms such as cognitive deficits in hippocampal-dependent spatial memory, depression and anxiety.

There are various cellular and molecular factors underlining these post-stroke psychiatric symptoms. Glutamatergic signalling may explain hippocampal vulnerability leading to spatial memory deficits, depression, and anxiety; as hippocampal interneurons are more resistant to excitotoxic insults compared to pyramidal cells, due to their glutamate receptor subunit composition (Kovalenko et al., 2006). Ischemia causes global increases in extracellular glutamate (Nishizawa, 2001), resulting in the reorganization of its receptor's subunits throughout hippocampal synapses (M. Chen et al., 2008; Z. Chen et al., 2014). These glutamatergic changes disrupt hippocampal synaptic plasticity or LTP, which is believed to underlie cognitive processes such as learning and memory. Emotional regulation may also be affected as abnormal hippocampal structure and function are often observed in depression and anxiety (Chan et al., 2016).

1.1.3 Gamma Oscillation Desynchrony in Ischemic Stroke

Network oscillations can be described as the electrical interaction and synchronous firing of spatially distinct excitatory and inhibitory neurons. These oscillations range from 0.05-500 Hz, which are further separated into smaller ranges that mediate specific psychophysiological functions. The two most prevalent ranges in the hippocampus are theta oscillations between 1-25 Hz and gamma oscillations between 25-140 Hz. The latter is generated from either the entorhinal cortex feeding into the dentate gyrus or the CA1-CA3 region (Csicsvari, Jamieson, Wise, & Buzsaki, 2003). Gamma oscillations are responsible for cortical-hippocampal circuit-dependent cognition and its ensuing cognitive processes such as attention, learning, and memory (Colgin & Moser, 2010). As network oscillations relate to ischemic stroke, a recent comprehensive review stated that ischemia leads to rises in low frequency and drops in high frequency oscillations; or specifically a decrease in the alpha to delta oscillation ratio (Moyanova & Dijkhuizen, 2014). Whether this ischemia-induced oscillatory pattern specifically applies to the hippocampus remains unclear. Currently, there are no studies linking changes in hippocampal synaptic plasticity, hippocampal gamma oscillations and behaviour in post-stroke conditions.

1.1.4 Hemispheric Differences in Ischemic Stroke

A unilateral ischemic stroke may initiate different cellular mechanisms in the ipsilateral and contralateral brain regions. This is clearly demonstrated in the motor cortex, where compensatory synaptic plasticity in the contralesional motor cortex allows for the relocalization of lost functions (Caleo, 2015). Functional neuroimaging studies have demonstrated enhanced contralateral activity immediately after a stroke (up to 10 days) followed by increased activity in ipsilateral regions during the chronic stages of stroke recovery (Marshall et al., 2000; Ward, Brown, Thompson, & Frackowiak, 2003). Post-stroke hemispheric differences are also apparent

in the prefrontal cortex and hippocampus (Madinier et al., 2013). It was found that pro-brain-derived neurotrophic factor (pro-BDNF) levels vary between hemispheres throughout the month following an ischemic stroke (Madinier et al., 2013). Not only does BDNF maintain synaptic plasticity, (Lu, Nagappan, & Lu, 2014), but it has been shown to be neuroprotective against oxygen and glucose deprivation (Van Kanegan et al., 2014). In an effort to equalize function between the hemispheres following a unilateral stroke, non-invasive neuromodulation has been used to either inhibit over-compensating contralateral regions or enhance insufficient ipsilateral regions (Di Pino et al., 2014; Grefkes & Ward, 2014).

1.2 Post-Stroke Behavioural Changes

1.2.1 Post-Stroke Depression

Post-stroke depression (PSD) occurs in 30-35% of stroke patients as it is one of the most common stroke-associated psychiatric complications (Lenzi, Altieri, & Maestrini, 2008). Patients suffering from PSD have higher mortality rates during rehabilitation compared to those who are not depressed. Like major depression, PSD is treated with antidepressants such as selective serotonin reuptake inhibitors and tricyclic antidepressants. In a recent study involving 1450 ischemic stroke patients, more than two thirds of those who were depressed (67.9%) were unresponsive to antidepressants (El Husseini et al., 2012). Other approved therapies such as neuromodulation in the form of non-invasive brain stimulation (NIBS) may be effective in these patients (Lenzi et al., 2008). For example, repetitive transcranial magnetic stimulation (rTMS) delivering frequencies higher than 20 Hz is regarded as a useful intervention for stroke-induced apathy (Sasaki et al., 2017). The unique pathophysiology of PSD provides itself as an opportunity for delineating the therapeutic mechanism of NIBS within this frequency range.

There are multiple pathophysiological factors or mechanisms within PSD. Lesion type, size and location are among the neuroanatomical factors. Pertaining to lesion location, there is conflicting data on whether it is predictive of the depressive symptoms that may result (Aben et al., 2006; Caeiro, Ferro, & Figueira, 2012; Snaphaan, van der Werf, Kanselaar, & de Leeuw, 2009). Other pathophysiological factors include: abnormal monoamine and glutamate signalling; neuroinflammation; stress on the hypothalamic-pituitary-adrenal axis; and reduced neurogenesis (Feng, Fang, & Liu, 2014). All of these factors are associated with the hippocampus, which is the brain region responsible for memory-dependent mood regulation. There is also evidence that PSD patients have very distinct patterns of hippocampal gamma oscillations compared to healthy individuals (Fitzgerald & Watson, 2018). However, it is difficult to generalize these patterns as they depend on the patient's cognitive state during the measurement, as well as the specific hippocampal region or cell population from which the measurements are taken.

1.2.1 Post-Stroke Anxiety

Approximately 20-25% of stroke patients experience anxiety. A meta-analysis of 13 studies including data from 2408 patients demonstrated a strong association between post-stroke anxiety (PSA) and PSD (Wright, Wu, Chun, & Mead, 2017). It is easy to imagine that many patients suffering from both psychiatric conditions are singularly prescribed antidepressants. Unlike depression, which tends to focus on loss, anxiety is often future oriented. In a recent study, phobic anxiety was found to be more common compared to generalized anxiety disorder in stroke patients (Chun, Whiteley, Dennis, Mead, & Carson, 2018). Aside from antidepressants, PSA patients may also be prescribed benzodiazepines or alpha-delta calcium channel convulsants (Farach et al., 2012). Currently, there are no neuromodulation studies that solely focus on PSA without the presence of PSD. However, rTMS delivering 20 Hz was found to significantly improve

symptoms in non-stroke patients with generalized anxiety disorder (Dilkov, Hawken, Kaludiev, & Milev, 2017).

Anxiety arises from dysregulations in limbic structures such as the amygdala, which generates emotional and fear-related memories. The amygdala is heavily connected to cortical regions, as it receives inputs from the hippocampus, thalamus, and hypothalamus (E. I. Martin, K. J. Ressler, E. Binder, & C. B. Nemeroff, 2009). The hippocampus has tonic inhibitory control over the hypothalamic-pituitary axis. However, ischemic stroke presents as a stressor that overrules this tonic inhibition, leading to glucocorticoid secretion that exacerbates neuronal damage (Radak, Resanovic, & Isenovic, 2014). As it relates to network oscillations, anxiety-related stimulus is associated with strong gamma oscillations from the visual cortex, fusiform gyrus, amygdala, and hippocampus (Albrecht, Caliskan, Oitzl, Heinemann, & Stork, 2013; Schneider et al., 2018). There are no studies measuring gamma oscillations in humans or animals experiencing PSA. However, stroke-induced disruptions in gamma oscillations likely affect communication between the hippocampus and medial prefrontal cortex, which regulates anxiety in the form of theta-gamma oscillation coupling (Adhikari, Topiwala, & Gordon, 2010; Khemka, Barnes, Dolan, & Bach, 2017; Padilla-Coreano et al., 2016).

1.2.3 Post-Stroke Cognitive Impairment

A cross-sectional study involving 10 countries and 6080 ischemic stroke patients suggested that more than 30% of these patients experienced cognitive impairment at some point throughout the five years following their stroke (Rist et al., 2013). The two most common forms of post-stroke cognitive impairment are aphasia and hemispatial neglect. Deficits in attention, learning, working memory, visual perception, and executive function (i.e. decision making, organization, problem solving) may also occur due to ischemic strokes (Gottesman & Hillis, 2010). Moreover, spatial

memory deficits are more frequent in right-hemispheric compared to left-hemispheric patients (De Renzi, Faglioni, & Previdi, 1977). There are an increasing number of studies using transcranial magnetic stimulation (TMS) to enhance cognition in not only those suffering from neurological and psychiatric disorders, but also in healthy individuals (Luber & Lisanby, 2014). Studies involving humans and animals have shown that frequencies in the 10-20 Hz range are effective in improving aspects of cognition such as working memory following an ischemic stroke (Guo, Lou, Han, Deng, & Huang, 2017; B. R. Kim, Kim, Chun, Yi, & Kwon, 2010).

Post-stroke cognitive impairments manifest from a series of highly heterogenous pathological events (Brouns & De Deyn, 2009; Kalaria, Akinyemi, & Ihara, 2016). It is likely that disruptions in synaptic plasticity and gamma oscillations are products of these pathological events. There are a couple anatomical generators of gamma oscillations in the hippocampus. Outside of the hippocamps, slow gamma oscillations ranging from 25-30 Hz are generated from the entorhinal cortex. This entorhinal cortex provides or encodes spatial information (Hafting, Fyhn, Molden, Moser, & Moser, 2005), which is then stored in the CA3 region of the hippocampus (Brun et al., 2002; Steffenach, Sloviter, Moser, & Moser, 2002). Altogether, oscillations from these regions provide a mode of input to the CA1 (Colgin et al., 2009). Optogenetic inhibition of the entorhinal-hippocampal circuit reduces gamma oscillation synchrony, resulting in impaired execution during a spatial memory task (Yamamoto, Suh, Takeuchi, & Tonegawa, 2014). Thus, it is conceivable that stroke-induced disruptions in these circuits could also lead to hippocampal-dependent spatial memory impairments.

1.3. Mechanisms in PVD

1.3.1. Introduction to PVD

Pial Vessel Disruption (PVD) is a focal cortical ischemic stroke model that is conducted in rats. It entails a 5 mm diameter craniotomy on the right and rostral side of the bregma. The class I large-sized pial vessel gives rise to class II medium-sized pial vessels, which eventually penetrate the cerebral cortex. In PVD, a few of these medium-sized pial vessels are permanently disrupted, causing a non-reperfusion injury (Hua & Walz, 2006). Within the next two days, the 1 mm^3 ischemic lesion becomes filled with both infiltrating and resident immune cells (Cayabyab, Gowribai, & Walz, 2013; K. Wang & Walz, 2003). Over the next 21 days, this region becomes a fluid-filled lacuna-like cavity that is encapsulated by reactive astrocytes (Hua & Walz, 2006; K. Wang & Walz, 2003). Moreover, resident microglia become activated and secrete matrix metalloproteinase-2 and -9, which break down the endothelial cells of the blood-brain barrier. This allows peripheral immune cells, such as lymphocytes, macrophages, and neutrophils, to infiltrate the brain parenchyma and exacerbate neuroinflammation (Cayabyab et al., 2013; Fan, Lo, & Wang, 2013; Wei et al., 2013). PVD is a small vessel stroke model with unique neuroinflammatory and neurodegenerative properties.

1.3.2 Adenosine-Mediated Glutamatergic Modulation in PVD

Adenosine is a purine nucleoside with major neuromodulatory mechanisms. It is comprised of an adenine molecule attached to a ribose sugar that has the potential to be phosphorylated. Adenosine can bind to four G-protein-coupled adenosine receptor subtypes known as A1, A2A, A2B, and A3 (Collis & Hourani, 1993; Fredholm, Chen, Cunha, Svenningsson, & Vaugeois, 2005). Its downstream signalling effects normal neuronal and glial functions (Fredholm et al.,

2005), motor functions (El Yacoubi et al., 2000), executive functioning (de Mendonca & Ribeiro, 1997), feeding (Lee, Li, Xi, Suh, & Martin, 2005), sleeping (Fredholm et al., 2005), and natural aging processes (Castillo et al., 2009; Costenla, Cunha, & de Mendonca, 2010). Due to adenosine's basal inhibitory tone in the hippocampus, it has always been thought to be neuroprotective in the excitotoxic conditions following ischemia (Cunha, Canas, Oliveira, & Cunha, 2006; Rudolphi, Schubert, Parkinson, & Fredholm, 1992; Sebastião, de Mendonça, & Ribeiro, 2001). However, recent studies have revealed its neurodegenerative potential through prolonged A1R activation in ischemic stroke (Z. Chen et al., 2014).

Aside from neuroinflammation at the immediate lesion site, PVD causes global increases in adenosine signalling that is matched by hippocampal neurodegeneration as soon as 48 hours after the ischemic stroke (Z. Chen et al., 2014). In both the ipsilateral and contralateral hippocampus, surface and total lysate expressions of A2AR are upregulated, while A1R levels are downregulated following PVD (Z. Chen et al., 2014). It was also suggested that A1R and A2AR signalling may be linked via serine/threonine protein kinase CK2 (Stockwell, Jakova, & Cayabyab, 2017). As such, PVD leads to upregulation of A2AR (Z. Chen et al., 2014) and downregulation of CK2 (Chen & Cayabyab, unpublished). CK2 normally contributes to A2AR desensitization rate (Rebholz et al., 2009), so the downregulation of CK2 is expected to mediate the observed A2AR upregulation during PVD.

Another component in this neurodegenerative pathway is adenosine-mediated glutamatergic modulation. Excitotoxic neurodegeneration predominantly occurs through the N-methyl-D-aspartate (NMDA) receptor of glutamate. However, A1R signalling was also found to affect the surface expression of two AMPA receptor subunits, GluA1 and GluA2 (Z. Chen et al., 2014; Stockwell, Chen, Niazi, Nosib, & Cayabyab, 2016). PVD downregulates A1R and

upregulates A2AR, leading to the internalization of GluA1 and GluA2 in both the ipsilateral and contralateral hippocampus (Z. Chen et al., 2014). Moreover, this glutamatergic modulation, specifically through GluA1, was found to be dependent on protein phosphatase (PP) activation as adenosine-mediated glutamate receptor internalization was prevented by various PP inhibitors (Stockwell et al., 2016). A diagram illustrating all of the speculated signalling proteins and pathways involved in ischemia- or PVD-induced A1R and A2AR crosstalk, as well as adenosine-mediated AMPAR modulation was recently published (Stockwell et al., 2017). Aspects of these pathways initiated by PVD may be therapeutic targets of GBOs delivered by LFMS.

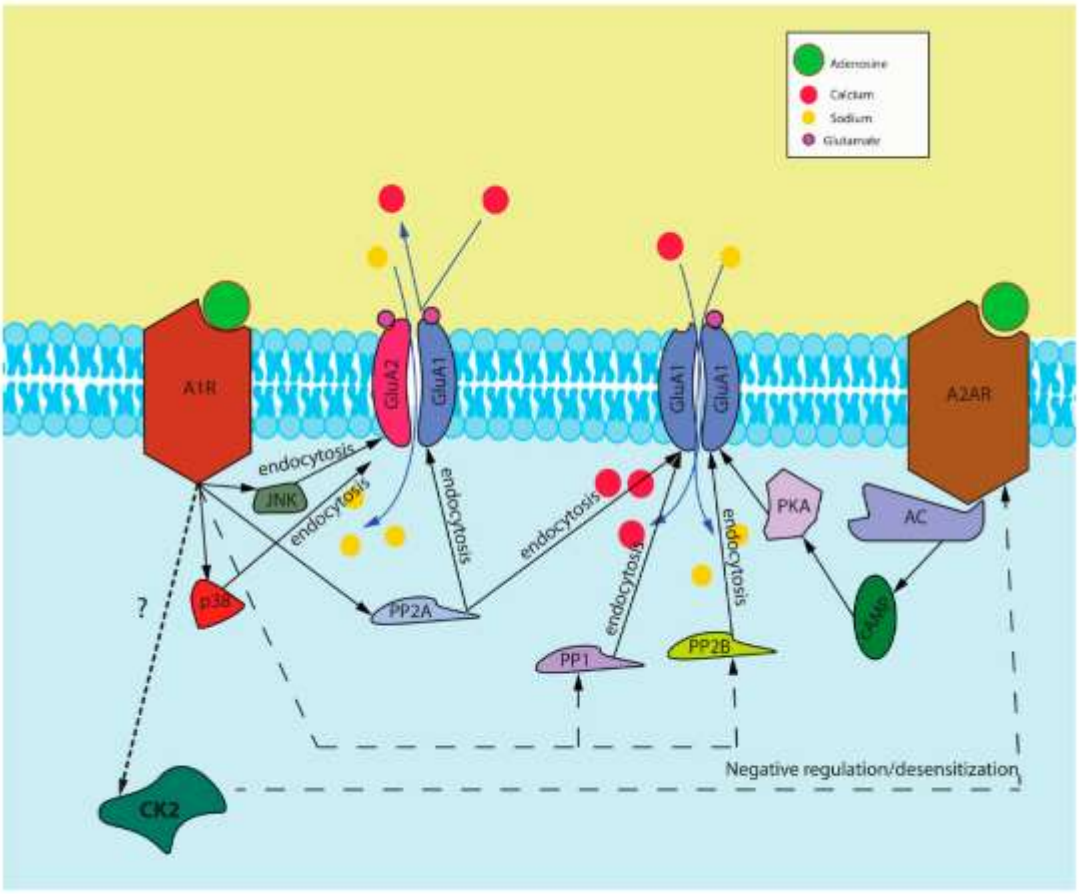

Figure 1.1 Proposed signalling pathway induced by A1R and A2AR activation following ischemia or PVD (Stockwell et al., 2017).

1.4 LFMS

1.4.1 Introduction to LFMS

LFMS is a subthreshold form of rTMS that has predominantly been investigated as a novel treatment for depression. Unlike rTMS, LFMS delivers lower electric field strengths that are less than 1 V/m (Shafi, Stern, & Pascual-Leone, 2014). These strengths cannot evoke action potentials; however, they may still affect synapses through dendritic excitability. In one study, field strengths of 1 V/m changed the membrane potential of a dendrite by 10 mV (Tranchina & Nicholson, 1986). LFMS operates in various magnetic parameters by adjustments in wave shape and temporal pattern. For example, the wave shape may be linear or uniform, while the magnetic stimulation may occur continuously or in pulses. Wave shape and direction targets specific cellular populations, while temporal pattern determines overall excitatory or inhibitory effects on synapses. The future of LFMS treatment entails matching these parameters to the desired electrophysiological effect within specific neurological and psychiatric disorders.

Another key difference between rTMS and LFMS is spatial resolution. LFMS consists of coils that surround the entire scalp, simultaneously exposing all brain regions to the electromagnetic stimulation (Shafi et al., 2014). Mood and cognition are regulated through multiple brain regions. Therefore, targeting the neural network desynchronies of a single brain region may not be the most effective therapeutic approach in psychopathology. Despite this reasoning, there are many conflicting reports on the advantages of unilateral versus bilateral neuromodulation. In one study, bilateral rTMS was more effective compared to its unilateral rTMS for improving bipolar depression (Kazemi et al., 2016). As it pertains to ischemic stroke, rTMS delivering a frequency of 10 Hz and positioned perpendicular to the cortex and approximately 5

mm right from the bregma, enhanced hippocampal neogenesis and suppressed apoptosis, thereby improving cognition in rats that had undergone middle cerebral artery occlusion (Guo et al., 2017).

1.4.2 Studies on LFMS to Date

The earliest LFMS study serendipitously occurred when a 20-minute magnetic stimulation with echo-planar magnetic resonance spectroscopic imaging (EP-MRSI) rapidly elevated mood in bipolar patients (M. L. Rohan et al., 2014). Similar degrees of mood elevation were observed in a subsequent study using the same stimulation parameters but involving patients with major depression disorder and bipolar disorder (M. L. Rohan et al., 2014). In this study, field penetration calculations revealed that the strongest magnetic fields were experienced by the prefrontal and orbitofrontal cortices (M. L. Rohan et al., 2014). This makes sense because dendritic excitability within neuronal layers five and six of the cortex greatly affect mood due its complex networks and inputs to subcortical regions such as the hippocampus and amygdala (Ledergerber & Larkum, 2010; Spruston, 2008). Another more recent study found that when MDD (Major Depressive Disorder) patients received LFMS in the gamma oscillation range of 7.5-12.5 Hz, their mood elevations were associated with a significant increase in serum brain-derived neurotrophic factor (BDNF), a neurotrophic factor critical for synaptic plasticity underlying e (Lu et al., 2014; Xiao et al., 2018). BDNF (Xiao et al., 2018).

LFMS has also recently been applied to Alzheimer's Disease (AD) models. As it relates to depression, up to 50% of AD patients experience depressed mood (Modrego, 2010) along with significant cognitive and memory deficits. In one study, applying LFMS for 40 minutes/day throughout eight weeks drastically attenuated amyloid β (Aβ) accumulation, restored hippocampal LTP, and improved cognition in amyloid precursor protein/presenilin-1 (5XFAD) mice (Zhen et al., 2017). In another study using 5FAX mice, gamma oscillations were optogenetically entrained

in the fast-spiking parvalbumin-positive interneurons. These entrainments induced genes associated with the morphological transformation of microglia, resulting in the co-localization of activated microglia and Aβ (Iaccarino et al., 2018). The question remains whether LFMS normalizes the electrophysiological aspects of AD, thereby restoring cellular and molecular pathology, or vice versa.

1.5 Hypothesis

It remains unclear whether GBOs delivered by LFMS can alleviate the emotional and cognitive impairments that occur following a focal cortical ischemic stroke. PVD is a non-reperfusion hypoxic lesion that initiates neuroinflammation at the immediate lesion site (Cayabyab et al., 2013; K. Wang & Walz, 2003), as well as synaptic depression and secondary neurodegeneration in the hippocampus (Z. Chen et al., 2014). At the molecular level, PVD causes the release of adenosine leading to persistent A1R stimulation and subsequent remodeling of both adenosine and glutamate receptor subtypes. Hippocampal gamma oscillations are likely disrupted following PVD. The causal order in which these events occur remains unclear. Nonetheless, LFMS aims to resynchronize hippocampal gamma oscillations to improve the emotional and cognitive impairments that occur as a result of multiple pathological events. While LTP underlies learning and memory at the molecular level, gamma oscillations are considered the larger-scale phenomenon that occurs during these higher cognitive processes. Thus, gamma oscillations are dependent on LTP, which heavily relies on neuronal viability and function. Neuroinflammation and neurodegeneration determine this viability. The Y-maze, Open Field Test (OFT), and Forced Swim Test (FST) were conducted to measure the improvements in hippocampal-dependent spatial memory, anxiety, and depression, respectively. The chemically-induced LTP (cLTP) protocol confirmed whether resynchronizing hippocampal gamma oscillations reversed adenosine-

mediated glutamatergic signalling to improve LTP. Finally, Propidium Iodide (PI) was used to quantify non-discriminant cell death, while Fluoro-Jade C (FJC) was stained for neurodegeneration in the hippocampus. Altogether, GBOs delivered by LFMS are hypothesized to be helpful in focal cortical ischemic stroke.

Chapter 2: Methods

2.1. Ethics Statement

All animals were treated according to guidelines of the Canadian Council for Animal Care (CCAC) under the supervision of the University of Saskatchewan Committee on Animal Care and Supply under the animal protocol approval number 20070090.

2.2. Stereotaxic Surgery

Male sprague dawley rats of approximately eight weeks of age were anesthetized with <2% isoflurane immediately after which they were subcutaneously injected with 0.03mL/kg of buprenorphine for pain management. For the PVD surgery, rats then underwent a 5 mm-diameter craniotomy on the right and rostral side of the bregma adjacent to the coronal and sagittal sutures. Once the dura was peeled back, Class II pial vessels were cut or permanently disrupted using fine-tipped forceps. Bleeding was controlled with ice-cold saline. The skull piece was then placed back, and the wound was sutured. Sham rats received the same treatment with dura removal but no vessel disruption.

2.3. LFMS Treatments

Rats were placed in a 30 x 15 x 15 cm mouse cage to be set up in the LFMS machine. For the Sham-LFMS treatment, the machine was plugged in and turned on, however, the stimulation was not initiated. For the LFMS treatment, the machine was turned on and the stimulation was initiated. Throughout the 20-minute stimulation, the electromagnetic waves occurred for two seconds every four seconds of rest. Throughout these two seconds, the wave pattern switched back and forth between Uniform and Linear patterns. The frequency of the stimulation was 40 Hz and

the electromagnetic field strength was approximately 1 V/m. Moreover, the stimulation was applied to the entire body, during which rats roamed freely in their cages.

2.4. Behaviour Testing

2.4.1 Y-maze

The Y-maze tests rodent's innate curiosity to explore spatially novel areas. It presents no negative or positive reinforcers and is minimally stressful for the rodents (Conrad, Galea, Kuroda, & McEwen, 1996). Success in this behaviour test is associated with hippocampal-dependent spatial memory, while poor Y-maze performance can be indicative of abnormal hippocampal pyramidal cell and dendrite networks (Conrad et al., 1996). The Y-maze was used to determine whether three LFMS treatments over three days improved PVD-induced damage to hippocampal-dependent spatial memory.

Y-maze apparatus consists of three arms that are joined by a triangle-shaped center to form a "Y" shape. Each arm has a rectangular base that is 45 x 12 cm, and all areas of the maze are surrounded by 35 cm tall walls. In the first trial, one of the three arms were blocked off. Rats were then placed in the maze for 15 minutes and free explore the start arm and the old arm, but not the blocked off novel arm. After the first trial, rats were placed back in their cages for a 90-minute break. In the second trial, rats were placed in the maze for five minutes and free to explore all arms including the recently unblocked novel arm. For both trials, there were spatial cues on the walls outside the maze for rats to easily view throughout their exploration periods. A video camera was used to record both trials. The Y-maze was the first of three behaviour tests conducted on the third experimental day.

A total of 48 rats underwent the Y-maze. There were 12 rats in each of the four treatment groups (n=12). This n-value is typical for seeing significant differences in behaviour studies on rats. The treatments of the rats were unknown or blinded throughout the Y-maze testing and subsequent analysis to minimize observer bias.

The video-tracking software, EthoVisionXT (Noldus) was used to automatically score the following: time spent in the start arm (s), time spent in the old arm (s), time spent in the novel arm (s), total distance travelled (cm), and velocity of movement (cm/s). These scores were determined for the second 5-minute trial. Time spent in each of the arms were calculated as a percentage of the total trial time. GraphPad Prism 6.0 (GraphPad) was used to construct all the graphs that were presented as a mean + SEM for each of the four treatment groups. GraphPad InStat version 6.0 (GraphPad) was used to apply a one-way ANOVA and a Tukey Kramer *post-hoc* test to determine statistical significance.

2.4.2 Open Field Test

Anxiety levels which may affect a rodent's willingness to explore an unfamiliar environment can be measured by the open-field test (OFT). The tendency of rodents to travel close to the walls and not enter the center, lit areas of the OFT apparatus is termed as thigmotaxis. It is unclear which brain regions mediate the specific behaviours within the OFT. Multiple regions and networks are likely involved, including the limbic areas controlling emotionality and fear, and higher neocortical regions controlling exploration and motor activity (Elizabeth I. Martin, Kerry J. Ressler, Elisabeth Binder, & Charles B. Nemeroff, 2009). Aside from anxiety, the OFT can be used to measure locomotion. In the current study, OFT was used to determine how LFMS affects emotional and physical functioning following PVD.

The OFT apparatus is a 56 x 56 cm square-shaped field surrounded 57 cm tall walls. The bright light that shines directly above the maze causes the 280 x 280 cm center square to be the brightest and most exposed area of the field. Rats were initially placed in this center square and free to explore the entirety of the field for 15 minutes. A video camera was used to record their behaviour. The open-field test was conduced after the Y-maze on the third day of experimentation.

A total of 48 rats underwent the OFT. There were 12 rats in each of the four treatment groups (n=12), which is the expectant number for seeing significant differences in behaviour studies on rats. To best eliminate bias, the treatments of the rats were unknown or blinded throughout the OFT testing and its subsequent analysis on EthoVisionXT.

EthoVisionXT (Noldus) was used to automatically score the following: center square entries, center square duration (s), distance travelled (cm), and velocity of movement (cm/s). All graphs were constructed using GraphPad Prism 6.0 (GraphPad) where scores were presented as a mean + SEM for every treatment group. Statistical significance was assessed using GraphPad InStat version 6.0 (GraphPad) where a one-way ANOVA and a Tukey Kramer post-hoc test were applied.

2.4.2 Forced Swim Test

The forced swim test (FST) is behaviour test that measures depressive symptoms such as despair and learned helplessness. When rodents are first placed in water, they are expected to swim as vigorously as possible to escape this stressful situation (Yankelevitch-Yahav, Franko, Huly, & Doron, 2015). As time passes, they reach a point of helplessness and despair, which is reflected by immobility or moving just enough to balance and keep their heads above the water to breathe

(Yankelevitch-Yahav et al., 2015). The FST was used to determine whether LFMS alleviated depressive symptoms in rats that had undergone PVD.

The FST apparatus is a 30 x 30 x 60 cm rectangle-shaped acrylic glass container that is two-thirds filled with water of 25°C (Yankelevitch-Yahav et al., 2015). Rats were placed in the container for 10 minutes, during which their behaviour was recorded by a video camera. The FST was the last of three behaviour tests conducted on the third experimental day.

A total of 48 rats underwent the FST. There were 12 rats in each of the four treatment groups (n=12). As previously mentioned, this number is typical for seeing significant differences in behaviour studies on rats. It was unknown which rat belonged to which treatment group as they were being tested in the FST. This blinding continued throughout behaviour analysis using EthoVisionXT.

The video files were uploaded to EthoVisionXT (Noldus), which automatically scored for two activity statuses throughout the test. The highly active and inactive statuses were separated by threshold of 0.15% of the total activity. All graphs were constructed using GraphPad Prism 6.0 (GraphPad) where scores were presented as a mean + SEM for every treatment group. Statistical significance was assessed using GraphPad InStat version 6.0 (GraphPad) where a one-way ANOVA and a Tukey Kramer post-hoc test were applied.

2.5. Hippocampal Slice Preparation

Eight-week-old sprague dawley rats were anesthetized with halothane then quickly decapitated. The brains were excised then submerged in an ice-cold oxygenated high-sucrose dissection medium containing the following (in mM): 87 NaCl, 25 $NaHCO_3$, 25 glucose, 75 sucrose, 2.5 KCl, 1.25 NaH_2PO_4, 7.0 $MgCl_2$, and 0.5 $CaCl_2$ (Brust, Cayabyab, & MacVicar,

2007). Hippocampus-containing slices were taken at 400 µm thickness using a vibrating tissue slicer or vibratome (VTS1200S, Vibram Instruments, Germany). Slicing occurred in the same ice-cold oxygenated high-sucrose dissection medium as described above. For the next hour in room temperature, hippocampal slices were submerged in oxygenated artificial cerebral spinal fluid (aCSF) containing the following (in mM): 126 NaCl, 2.5 KCl, 2.0, MgCl2, 1.25 NaH2PO4, 26 NaHCO3, 10 glucose, 2.0 CaCl2 (Brust et al., 2007). Oxygenation was accomplished by continually aerating the solution with 95% O2/5% CO2.

2.6. Electrophysiology

Electrophysiological recordings from acute hippocampal slices are a way to measure the sensitivity of spontaneously evoked electrical signal transmissions to various neuronal manipulation such as pathologies and treatments. These recordings allow us to study synaptic plasticity (a measure of synaptic efficacy or synaptic strength), which could regulate the neurophysiological basis of learning and memory. Chemically-induced long-term potentiation (cLTP) mimics spontaneous LTP to allow measurements of maximally reaching and sustained field excitatory postsynaptic potentials (fEPSPs) throughout 1 hour. As such, the fEPSPs of healthy control slices are expected to be higher during both cLTP and washout periods compared to slices sustaining neurological injuries such as ischemic stroke and hypoxia.

Hippocampal slices were submerged in an electrophysiology recording chamber with constant perfusion of room temperature oxygenated aCSF (3 ml/min). The fEPSPs were evoked by orthodromic stimulation of the Schaffer collateral pathway using a bipolar tungsten stimulating electrode. These fEPSP signals were digitized at 10kHz using Digidata 1440A interface board and analyzed using Clampfit 9.0 (Axon Instruments, Foster City, CA). A recording microelectrode filled with aCSF was placed in the CA1 stratum radiatum.

Throughout each experiment, fEPSPs were evoked for 0.1 ms every 30 seconds. The stimulation amplitude for fEPSP was determined based on the maximum amplitude found for each hippocampal slice following a 20-minute equilibration period. It was then reduced until fEPSPs were approximately a third of the maximum value. The baseline recordings were for at least 10 minutes. A treatment of Forskolin (50 µM)/Rolipram (0.1 µM) was perfused in aCSF that lacked Mg^{2+}. Forskolin is an adenylyl cyclase (AC) activator, which ultimately increases extracellular cyclic adenosine monophosphate (cAMP) levels. Rolipram is a selective phosphodiesterase-4 inhibitor that prevents the breakdown of cAMP thereby increasing its extracellular levels. Collectively, forskolin and rolipram promote intracellular LTP mechanisms through cAMP. The cLTP induction was followed by a 1-hour washout period in aCSF that contained Mg^{2+}. Synaptic plasticity during the washout period was not NMDA-dependent as this receptor was blocked by Mg^{2+} provided by the aCSF solution. The fEPSP slopes were normalized to the mean of 10 sweeps (five minutes).

The n-values for the ipsilateral PVD & Sham-LFMS and PVD & LFMS treatment groups were 13 and four, respectively. The n-values for the contralateral PVD & Sham-LFMS and PVD & LFMS treatment groups were five and four, respectively. The n-value for the Naïve & LFMS treatment group was three. GraphPad Prism 6.0 (GraphPad) was used to construct all of the graphs, where %fEPSPs were presented as a mean + SEM for every treatment group. Statistical significance was assessed using GraphPad InStat version 6.0 (GraphPad) where a one-way ANOVA and a Tukey Kramer post-hoc test were applied.

2.7 Propidium Iodide Staining

Propidium iodide (PI) is a fluorescent marker for non-discriminant cell death. It cannot transverse cells that possess intact plasma membranes, therefore, it only binds to the DNA of dead

cells with damaged plasma membranes. Wavelengths between 400 nm and 600 nm (green light) excite PI molecules to emit red fluorescence between 600 nm and 700 nm. This marker was used to determine whether PVD-induced cell death can be prevented by three LFMS treatments.

A total of 12 rats (three rats per treatment group) were dedicated to PI staining. Fresh hippocampal slices were incubated for 1 hour in a solution containing room-temperature aCSF and 5µg/mL PI. The subsequent procedures were performed in the dark to prevent photobleaching. Following 1-hour incubation, slices were rinsed thoroughly in 1X Phosphate-buffered saline (PBS) then fixed in 4% paraformaldehyde (PFA) at 4°C overnight. The next day, slices were rinsed 3 x 15 minutes in 1 X PBS, then mounted on gelatin-coated microscope slides (VWR, USA) and sealed using Prolong Gold Antifade Reagent (Invitrogen, USA)

The slides containing PI-stained hippocampal slices were imaged using a Zeiss LSM700 laser scanning confocal microscope (Carl Zeiss, Germany). A green light (543 nm) was used to induce PI fluorescence. The 10x objective lens was used to image the whole hippocampus in consecutive pieces. The CA1 pyramidal neurons were imaged using a Zeiss Plan-Apochromat 63x/1.6 oil objective lens (Carl Zeiss, Germany). This lens captured z-stack images of 2 µm thickness at 200 µm depth into the hippocampus. Two z-stacks along the CA1 were taken per slice, which were then averaged using densitometry analysis.

The Zeiss Zen 2009 version 5.5 software (Carl Zeiss, Germany) yielded the data for densitometry analysis using ImageJ (NIH). As z-stack images towards the outer top and bottom of the hippocampal slice sustained the most damage from the slicing procedure, the inner-most 20 µm (~100 µm into the slice) segments were combined as a maximum intensity projection image. The mean intensity of this image was measured, averaged for each slice and treatment group, then normalized to the control group. Data was graphed as a percentage of the control group (100%)

for statistical analysis. Images collected from the 10x objective lens were assembled as montages of the whole hippocampus using Adobe Photoshop CS6 (Adobe Systems, Mountain View, CA).

GraphPad Prism 6.0 (GraphPad) was used to construct all of the graphs, where PI intensity was presented as a mean + SEM for every treatment group. Statistical significance was assessed using GraphPad InStat version 6.0 (GraphPad) where a one-way ANOVA and a Tukey Kramer post-hoc test were applied.

2.8 Fluoro-Jade C Staining

Fluoro-Jade C (FJC) is a fluorochrome derived from fluorescein that stains all degenerating neurons regardless of the mechanism of insult or neurodegeneration. The maximum excitation and emission wavelengths for FJC are 485 nm and 525 nm, respectively. Unlike PI, FJC was used to determine whether LFMS prevented or reversed neuronal death or neurodegeneration.

A total of 12 rats (three rats per treatment group) were used for FJC. All rats were first anesthetized, perfused, and their brains sliced. Rats were anesthetized with <2% isoflurane then a series of skin and diaphragm cuts exposed their hearts. As a needle infused 4% PFA into the left ventricle, the right atrium was cut to allow blood to flow out of the body. The PFA perfusion lasted for approximately 20 minutes. After the perfusion, the brain was removed and post-fixed in 4% PFA in 0.1 M PBS overnight. Brains were then stored in 30% sucrose (w/v) in 0.1 M PBS for an additional 3 days. Once the brains sunk to the bottom of the sucrose and PBS solution, they were frozen using solid carbon dioxide. Tissue Tek OCT mounting medium was used to mount the brain on a microtome (Leica Biosystems, Germany) for slicing. Slices were taken at 400 µm thickness then stored in Millonig's Phosphate Buffer at 4°C.

For the FJC staining process, the perfused hippocampal slices were first mounted on gelatin-coated microscope slides (VWR, USA). The mounted slices were then immersed in 70% ethanol, washed three times (one minute each time) with double-distilled water (ddH_20), and immersed in 0.06% KMNO4 for 15 minutes. The slices were then washed again in ddH20 (three times, one minute each time) and stained with 0.001% FJC (Millipore Bioscience Research Reagents) for 20 minutes. The subsequent steps were performed in the dark to prevent photobleaching. Slices were washed for the last time in ddH_20 (3 times, one minute each time) then dried in 4°C overnight. The mounted slices were rinsed in xylene and cover-slipped using Prolong Gold Antifade Reagent (Invitrogen).

A Zeiss LSM700 laser scanning confocal microscope (Carl Zeiss, Germany) was used to image the slides containing FJC-stained hippocampal slices. A green light (488 nm) was used to induce FJC fluorescence. The whole hippocampus was imaged in consecutive pieces using the 10x objective lens. Alternatively, the CA1 pyramidal neurons were imaged using a Zeiss Plan-Apochromat 63x/1.6 oil objective lens (Carl Zeiss, Germany). This lens captured z-stack images of 2 µm thickness at 200 µm depth into the hippocampus. Each slice provided two z-stacks along the CA1, which were then averaged using densitometry analysis.

Data was yielded through the Zeiss Zen 2009 version 5.5 software (Carl Zeiss, Germany), which was then densitometrically analysed using ImageJ (NIH). As z-stack images towards the outer top and bottom of the hippocampal slice sustained the most damage from the slicing procedure, the inner-most 20 µm (~100 µm into the slice) segments were combined as a maximum intensity projection image. The mean intensity was calculated for each image, and these values were averaged for each animal and treatment group. After each treatment group mean was normalized to the control group mean, data was graphed as a percentage of the control group

(100%). Images collected from the 10x objective were assembled as montages of the whole hippocampus using Adobe Photoshop CS6 (Adobe Systems, Mountain View, CA).

GraphPad Prism 6.0 (GraphPad) was used to construct all of the graphs, where FJC intensity was presented as a mean + SEM for every treatment group. Statistical significance was assessed using GraphPad InStat version 6.0 (GraphPad) where a one-way ANOVA and a Tukey Kramer post-hoc test were applied.

Chapter 3: Results

3.1 Behaviour Testing

3.1.1 LFMS on depressive behaviour measured by the FST

The earliest LFMS studies focused on rapidly improving mood in patients with bipolar and major depressive disorders (M. Rohan et al., 2004; M. L. Rohan et al., 2014). Depressed mood is not limited to psychiatric disorders. Nearly 30% of stroke survivors experience depression (Paolucci, 2008), yet there are currently no studies on GBOs or LFMS in the gamma frequency range being applied to PSD. To better understand the therapeutic mechanism of LFMS, rats that underwent PVD received three once-daily LFMS treatments. The FST was one of three behaviour tests conducted on the fourth day of the study. This test was conducted last to prevent its stresses from impacting the other two tests. As such, the GBOs delivered by LFMS was hypothesized to lessen helplessness and despair in rats experiencing depression following PVD.

LFMS drastically improved immobility scores in the FST. As expected, the PVD & Sham-LFMS group displayed the shortest latency to immobility (Figure 3.1a) and the longest time spent immobile (Figure 3.1a). These results demonstrate that PVD is a reliable model for studying the depressive behaviour that occurs as early as three days after an ischemic stroke. Compared to the PVD & Sham-LFMS group, the PVD & LFMS group spent significantly less time immobile (Figure 3.1b) and more time swimming or struggling before reaching immobility (Figure 3.1a). The exact mechanism by which GBOs improve depressive behaviour is unknown. Various parameters of NIBS have been found to be effective in depression. By understanding the mechanisms of these electrical, spatial, and temporal parameters, they can be used to target specific aspects and patterns of depressive behaviour

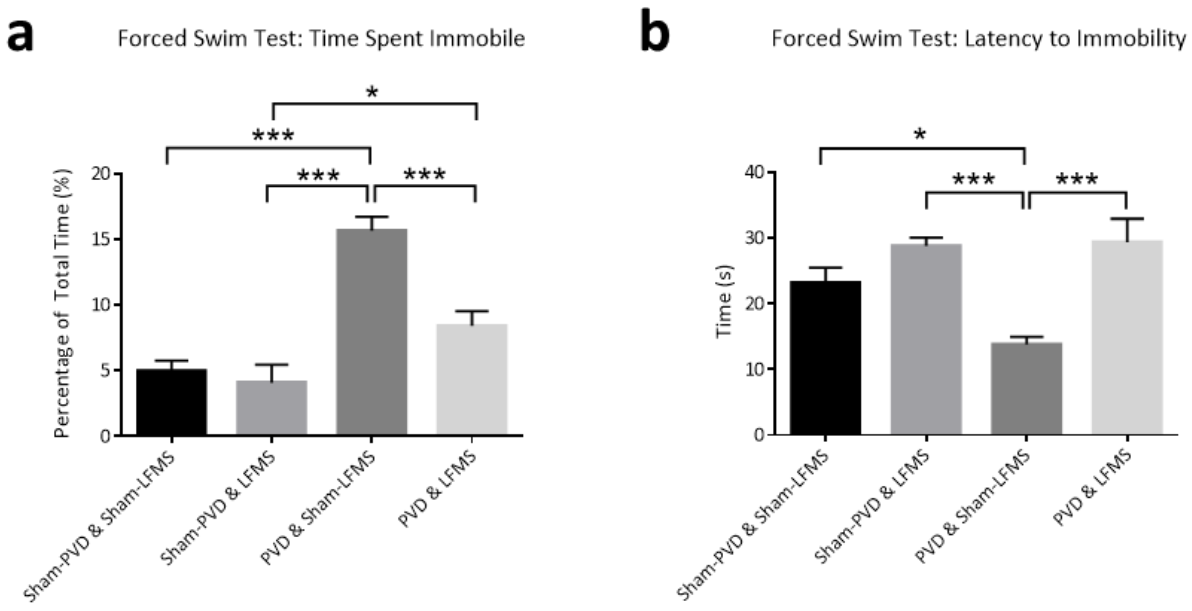

Figure 3.1 LFMS improved immobility scores indicating learned helplessness and despair in the PVD & LFMS group. (a, b) Rats were placed in a container of water for 10 minutes, and time spent immobile was calculated as a percentage of the total trial time. Latency to immobility was plotted as times in seconds. (a) The PVD & Sham-LFMS group displayed the largest percentage of time spent immobile compared to all other groups. LFMS treatment significantly decreased this percentage in rats that underwent PVD. (b) The PVD & Sham-LFMS group had the lowest latency to immobility score compared to all other groups. LFMS treatment significantly restored this latency to immobility. n=12 for each treatment group. n=12 for each treatment group. Values are shown as mean + SEM. Significance values: *= $p<0.05$, **= $p<0.01$.

3.1.2 LFMS on anxious behaviour measured by the OFT

Depression and anxiety often present together following a stroke (Schöttke and Giabbiconi, 2015). It has been previously shown that a single LFMS treatment improves both depressive and anxious behaviour in patients suffering from bipolar and major depressive disorders (M. L. Rohan

et al., 2014). This study gave reason for applying LFMS to post-traumatic stress disorder (M. Rohan, 2015). which is primarily an anxiety disorder involving depressive episodes (American Psychiatric Association, 2013). In order to characterize the effects of GBOs on PSA, the OFT was conducted after the Y-maze and before the FST on the fourth day of the current study. The stimulation was hypothesized to lessen anxiety-like behaviour thereby encouraging center square exploration in rats experiencing PSA.

There were no significant differences between any of the groups with regards to either center square entries of duration (Figure 3.2a, b, c, d, e, f). However, the PVD & Sham-LFMS group showed slightly decreased center square entries and duration compared to the Sham-PVD & Sham-LFMS group ($p=0.9424$) and the Sham-PVD & LFMS group ($p=0.0756$). These data trends are telling of anxious behaviour. The PVD & Sham-LFMS group displayed lower center square entries compared to the two LFMS groups; as well as the lowest center square duration compared to all other groups (Figure 3.2c, e, f). GBOs seemed to restore center square entries and duration in rats that underwent PVD (Figure 3.2d, e, f). A statistical power analysis will be able to calculate the number of n-values required to make these results significant. It must also be kept in mind that center square entries are a less reliable measure of exploratory behaviour. Rats may enter the center square while moving from wall to wall. All in all, LFMS may have a moderate anxiolytic effect on rats that underwent PSA.

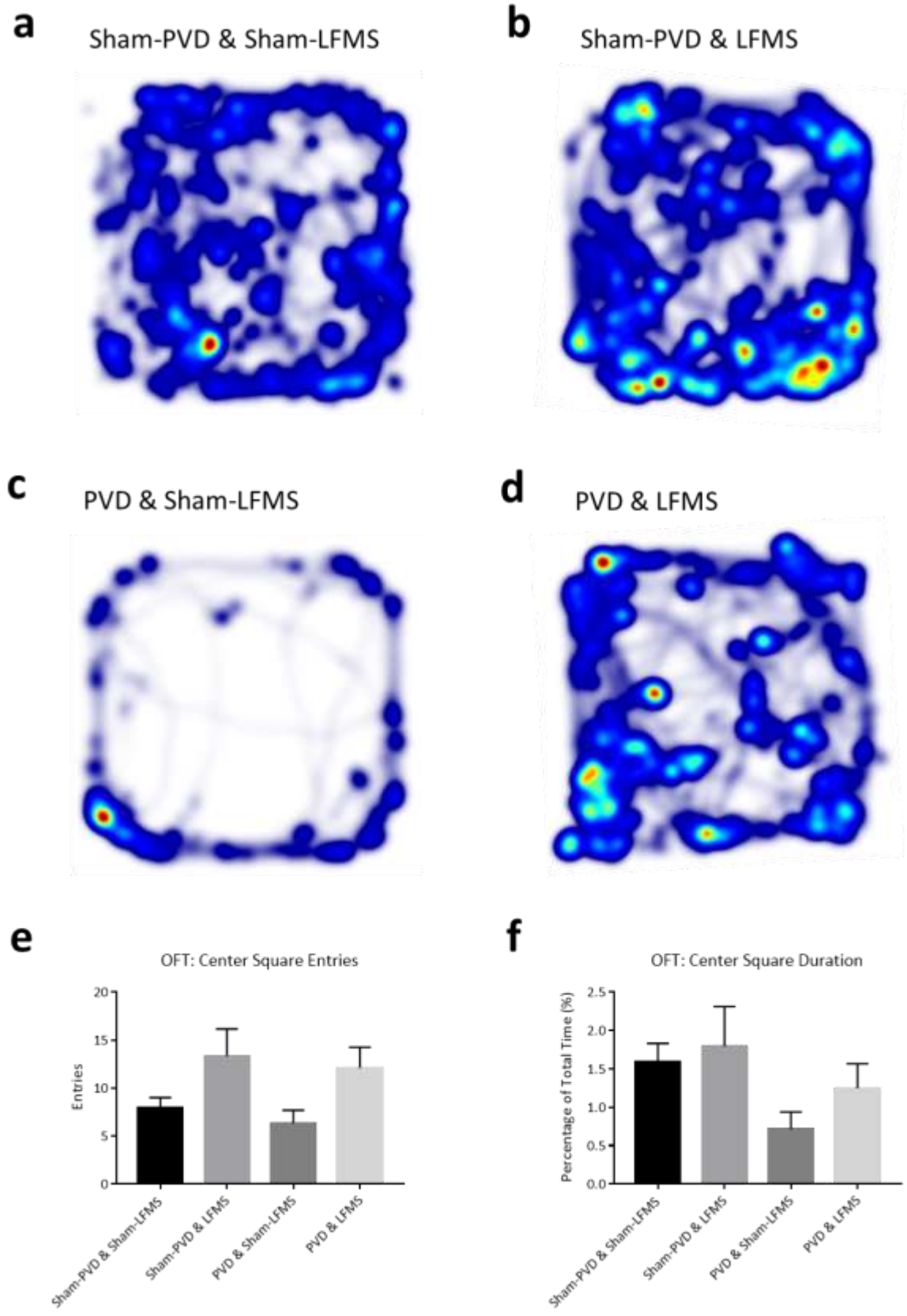
a
Sham-PVD & Sham-LFMS
b
Sham-PVD & LFMS
c
PVD & Sham-LFMS
d
PVD & LFMS
e
OFT: Center Square Entries
Entries
20
15
10
5
0
Sham-PVD & Sham-LFMS
Sham-PVD & LFMS
PVD & Sham-LFMS
PVD & LFMS
f
OFT: Center Square Duration
Percentage of Total Time (%)
2.5
2.0
1.5
1.0
0.5
0.0
Sham-PVD & Sham-LFMS
Sham-PVD & LFMS
PVD & Sham-LFMS
PVD & LFMS

Figure 3.2 LFMS seemed to restore center square entries and duration in the PVD & LFMS group. (a-f) Rats were placed in the brightly lit OFT for 15 minutes, during which they were free to explore. All durations were calculated as a percentage of the 15-minute trial. (c, e) Although the PVD & Sham-LFMS group entered the center square the least compared to the other groups, these comparisons were not significant. (c, e) The PVD & Sham-LFMS group displayed the lowest center square duration compared to the two Sham-PVD groups. (d, f) LFMS increased center square duration in the PVD & LFMS group, however, this increase was not significant. n=12 for each treatment group. n=12 for each treatment group. Values are shown as mean + SEM. Representative heat maps from each treatment group were acquired on EthoVision.

3.1.3 PVD and LFMS on locomotion measured by the OFT

It is unknown whether PVD or LFMS causes locomotive changes. Many stroke models do impair motor skills to some degree. However, the PVD model focuses on hippocampal functionality and one study was able to show that hippocampal lesioning does not affect the acquisition of a motor learning tasks (Gould et al., 2002). Nevertheless, it is important to rule out any PVD-induced motor impairments in order to properly interpret the other behaviour tests. As it pertains to LFMS, gamma oscillations have been linked to higher running velocities. For instance, faster running velocities were associated with large, systematic increases in the frequency of network oscillations ranging from the 30-120 Hz (Ahmed & Mehta, 2012). In the current study, mean velocity and distance travelled in the OFT were two measurements used to confirm whether PVD or LFMS significantly affected locomotion.

There were no differences in mean velocity or distance travelled between any of the groups (Figure 3.3a, b). As the 1-mm^3 PVD lesion does not penetrate deeper than the cerebral cortex, it was not expected to have a significant effect on motor skills. There was a trend where the Sham-

PVD & LFMS (p=0.054, p=0.5205) and PVD & LFMS (p=0.0564, p=0.5319) group moved faster compared to those that received Sham-LFMS (Figure 3.3a). These groups also covered more distance compared to the Sham-LFMS groups (p=0.2683, p=0.3508, p=0.9982, p=0.6775) (Figure 3.b). A statistical power analysis must be conducted to determine whether more n-values are required to solidify this trend. There is accumulating evidence that NIBS is therapeutic in stoke, as well as a variety of other neurological disorders involving motor deficits (Belci, Catley, Husain, Frankel, & Davey, 2004; Benninger et al., 2011; Freitas, Mondragon-Llorca, & Pascual-Leone, 2011; Webster, Celnik, & Cohen, 2006). As the focus of the current study is on post-stroke cognitive and emotional impairments, it can be confirmed that neither PVD nor LFMS have motor effects that may take away from these focuses.

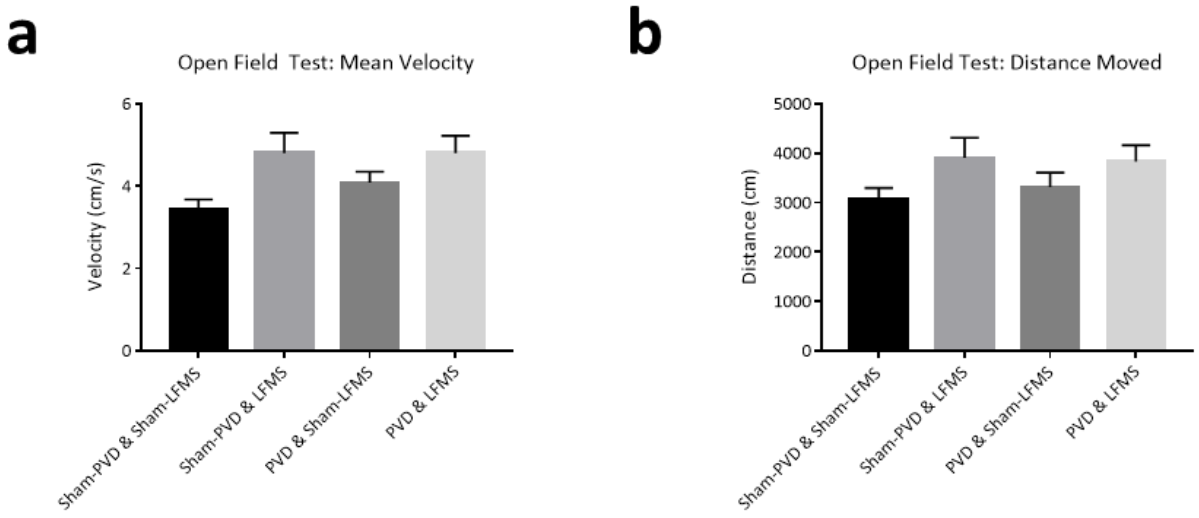

Figure 3.3 Locomotor activity measured by mean velocity and distance travelled was not affected by PVD, nor was it significantly enhanced by LFMS treatment. (a, b) Rats were placed in the brightly lit OFT for 15 minutes, during which they were free to explore. (A) Although both LFMS groups displayed higher mean velocities compared to the Sham-LFMS groups, these differences were not significant. (b) All distance scores resembled the trends in (a), where the

Sham-PVD & LFMS and PVD & LFMS groups travelled the most distance on average. n=12 for each treatment group. n=12 for each treatment group. Values are shown as mean + SEM.

3.1.4 LFMS on hippocampal-dependent memory measured by the Y-maze

Aside from depression and anxiety, ischemic stroke patients may also suffer from cognitive impairments related to episodic memory, working memory, attention and executive functioning (Dotson et al., 2014). The Y-maze was used to evaluate exploratory behaviour within the context of hippocampal-dependent spatial memory. It was the first of three behaviour tests conducted following the third and final LFMS treatment. This particular order of behaviour testing prevented the other two more stressful tests from impacting the rats' cognitive performance in the Y-maze. GBOs delivered by LFMS was hypothesized to restore novel arm duration, indicating improved hippocampal-dependent spatial memory in rats that had undergone PVD.

The only significant difference in this experiment was between the control, represented by the Sham-PVD & Sham-LFMS group, and the PVD & LFMS group in novel arm duration (Figure 3.4a, d, g). The PVD & Sham-LFMS group was the least able to distinguish the novel arm from the other arms, which makes sense because rats in this group sustained the worst neurological injury and received no treatment thereafter (Figure 3.4c, g). Despite the lack of significant differences between the two PVD groups in any of the arm durations, there was a trend where the LFMS group spent more time in the novel arm and less time in the old arm, indicating improved hippocampal-dependent spatial memory compared to its Sham-LFMS counterpart ($p=0.5259$) (Figure 3.4c, d, f, g). More n-values are required to better understand these results. Nonetheless, gamma oscillations have been shown to improve cognitive in other neurodegenerative models such Alzheimer's Disease (Mably & Colgin, 2018; Zhen et al., 2017).

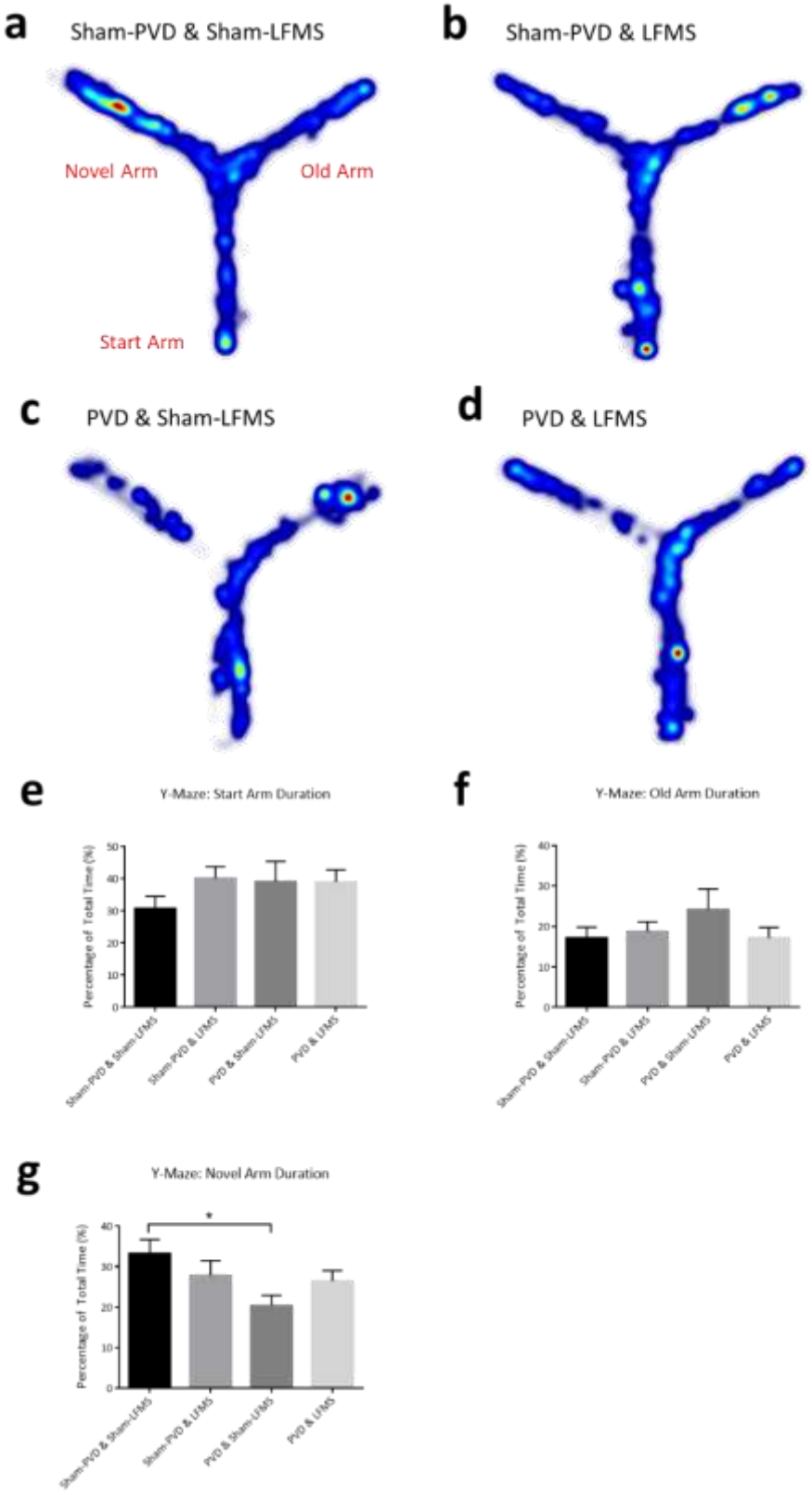
a
Sham-PVD & Sham-LFMS
Novel Arm
Old Arm
Start Arm
b
Sham-PVD & LFMS
c
PVD & Sham-LFMS
d
PVD & LFMS
e
Y-Maze: Start Arm Duration
Percentage of Total Time (%)
Sham-PVD & Sham-LFMS
Sham-PVD & LFMS
PVD & Sham-LFMS
PVD & LFMS
f
Y-Maze: Old Arm Duration
Percentage of Total Time (%)
Sham-PVD & Sham-LFMS
Sham-PVD & LFMS
PVD & Sham-LFMS
PVD & LFMS
g
Y-Maze: Novel Arm Duration
*
Percentage of Total Time (%)
Sham-PVD & Sham-LFMS
Sham-PVD & LFMS
PVD & Sham-LFMS
PVD & LFMS

Figure 3.4 LFMS did not significantly improve novel arm duration in the PVD & LFMS group. (a-g) After a 90-minute break, rats were placed back in the Y-maze for the second trial of five minutes. Arm durations were calculated as a percentage of the 5-minute trial. (c, g) The PVD & Sham-LFMS group generally spent the least amount of time in the novel arm compared to all other groups, especially the Sham-PVD & Sham-LFMS group. (a, g) There were no other significant differences between the groups. However, there was a trend where the PVD & LFMS group spent more time in the novel arm and less time in the old arm compared to the PVD & Sham-LFMS group. n=12 for each treatment group. n=12 for each treatment group. Values are shown as mean + SEM. Representative heat maps from each treatment group were acquired on EthoVision.

3.2 LFMS on hippocampal synaptic plasticity

As previously mentioned, the hippocampus is particularly vulnerable to ischemic stroke. This vulnerability may present as impairments in LTP or synaptic depression (Li et al., 2013). In the case of a unilateral hypoxic lesion, the ipsilateral and contralateral hippocampi (relative to the lesion) may exhibit different patterns of LTP. For the cLTP experiments, the PVD & Sham-LFMS and PVD & LFMS groups were further separated into ipsilateral and contralateral groups. An extra treatment group called “Naïve & LFMS” was also added. This group did not undergo any surgical intervention but still received the three once-daily LFMS treatments. The purpose of the Naïve & LFMS group was to assess how GBOs affect healthy controls. All in all, both PVD groups were expected to display hemispheric differences in LTP during the cLTP and washout periods. Moreover, the ipsilateral and contralateral PVD & LFMS groups were expected to resemble the Naïve & LFMS group more than its Sham-LFMS counterparts.

The contralateral PVD & Sham-LFMS group reached the highest fEPSPs during the cLTP compared to all other groups (Figure 3.5a, b, d, e). During washout, the contralateral PVD & Sham-

LFMS sustained LTP better than the ipsilateral PVD & Sham-LFMS group (Figure 3.5a, b, d, e). There were no differences in fEPSPs during either cLTP or washout amongst the PVD & LFMS groups (Figure 3.5a, c, d, e). The ipsilateral and contralateral PVD & LFMS group was also very similar to the Naïve & LFMS group throughout the experiment (Figure 3.5a, c, d, e). These results demonstrate that PVD causes major hemispheric differences in LTP, while GBOs equalize these differences to make both hemispheres resemble the Naïve & LFMS group. There have been NIBS studies with a similar goal, where they applied higher frequencies (>3 Hz) to the ipsilateral cortex to increase excitability and lower frequencies (≤1 Hz) to the contralateral cortex to decrease excitability (Kubis, 2016).

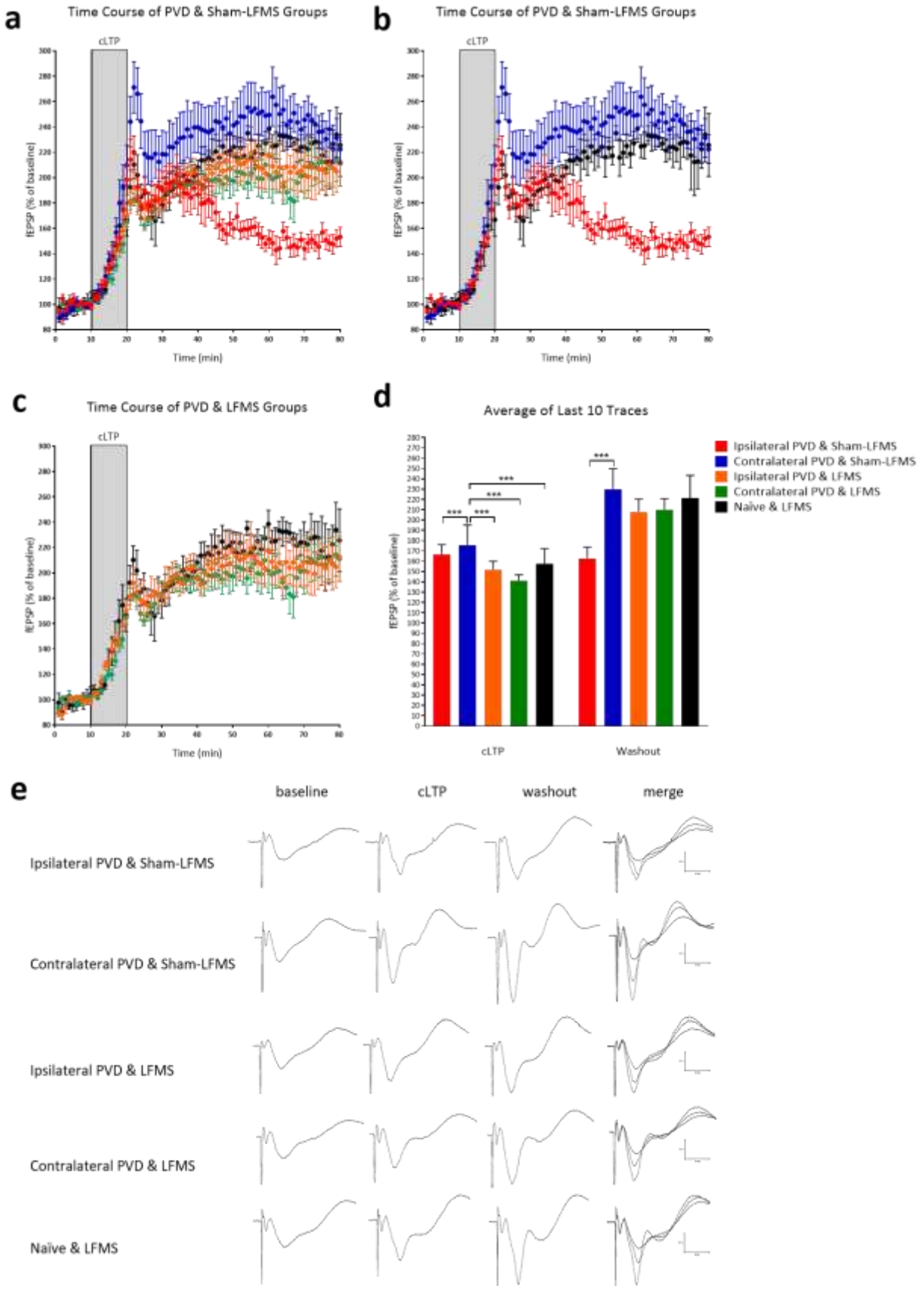
a
Time Course of PVD & Sham-LFMS Groups
cLTP
fEPSP (% of baseline)
Time (min)
b
Time Course of PVD & Sham-LFMS Groups
cLTP
fEPSP (% of baseline)
Time (min)
c
Time Course of PVD & LFMS Groups
cLTP
fEPSP (% of baseline)
Time (min)
d
Average of Last 10 Traces
fEPSP (% of baseline)
***
***
***
***
cLTP
Washout
Ipsilateral PVD & Sham-LFMS
Contralateral PVD & Sham-LFMS
Ipsilateral PVD & LFMS
Contralateral PVD & LFMS
Naïve & LFMS
e
baseline
cLTP
washout
merge
Ipsilateral PVD & Sham-LFMS
Contralateral PVD & Sham-LFMS
Ipsilateral PVD & LFMS
Contralateral PVD & LFMS
Naïve & LFMS

Figure 3.5 PVD and LFMS had different effects on synaptic plasticity in the ipsilateral and contralateral hippocampus. fEPSPs were evoked in the Schaffer collateral pathway while a recording electrode was placed in the CA1 stratum radiatum. A solution of Forskolin and Rolipram was perfused in aCSF. This cLTP induction was followed by a 1-hour washout period. (a, b, d, e) The contralateral PVD & Sham-LFMS group exhibited the highest fEPSPs during cLTP. This group better sustained LTP better than its ipsilateral counterpart throughout washout. Compared to the Naïve & LFMS group, the contralateral PVD & Sham-LFMS group reached higher potentials during cLTP but similarly sustained LTP during washout. (a, c, d, e) There were no differences in fEPSPs between the ipsilateral and contralateral PVD & Sham-LFMS group during either cLTP or washout. These groups exhibited fEPSPs that were similar to the Naïve & LFMS group all throughout the experiment. N varied from three to 13 for each treatment group. Values are shown as mean + SEM. Significance values: *= $p<0.05$, **= $p<0.01$. Trace images were produced using OriginLab.

3.3 LFMS on non-discriminant cell death in the hippocampus

Various neuroprotection studies have made the links between hippocampal cell viability, LTP, and cognition (Yabuki & Fukunaga, 2013; Yang, Yao, Chen, & Zhang, 2014). PVD causes changes in adenosine and glutamate signalling, leading to synaptic depression and neurodegeneration in the hippocampus (Z. Chen et al., 2014). PVD induces hypoxia leading to persistent A1R stimulation (Z. Chen et al., 2014). Therefore, both hypoxia and A1R agonism was shown to cause significant hippocampal cell death that was reversible by A1R antagonism (Stockwell et al., 2016). In the current study, hippocampal slices were incubated in Propidium Iodide for one hour before being fixed in paraformaldehyde, cover-slipped, and imaged using a Zeiss LSM700 laser scanning confocal microscope. Considering the behaviour and

electrophysiology data, GBOs were expected to differentially lessen cell death in the ipsilateral and contralateral hippocampus.

Ipsilateral to the lesion, LFMS significantly reduced red fluorescence or cell death in slices that sustained PVD injury (Figure 3.6a, c). Moreover, this reduction in cell death was comparable to the time control and Sham-PVD & LFMS (Figure 3.6a, c). Contralateral to the lesion, the PVD & Sham-LFMS group displayed much less cell death compared to its ipsilateral counterpart (Figure 3.6b, d). However, LFMS was still successful in significantly reducing contralateral cell death (Figure 3.6b, d). These hemispheric differences in hippocampal cell death support the electrophysiology data, where there are different synaptic plasticity mechanisms between the ipsilateral and contralateral hippocampus. More research must be done to delineate the mechanistic links between LTP and cell death in each hemisphere following PVD.

a

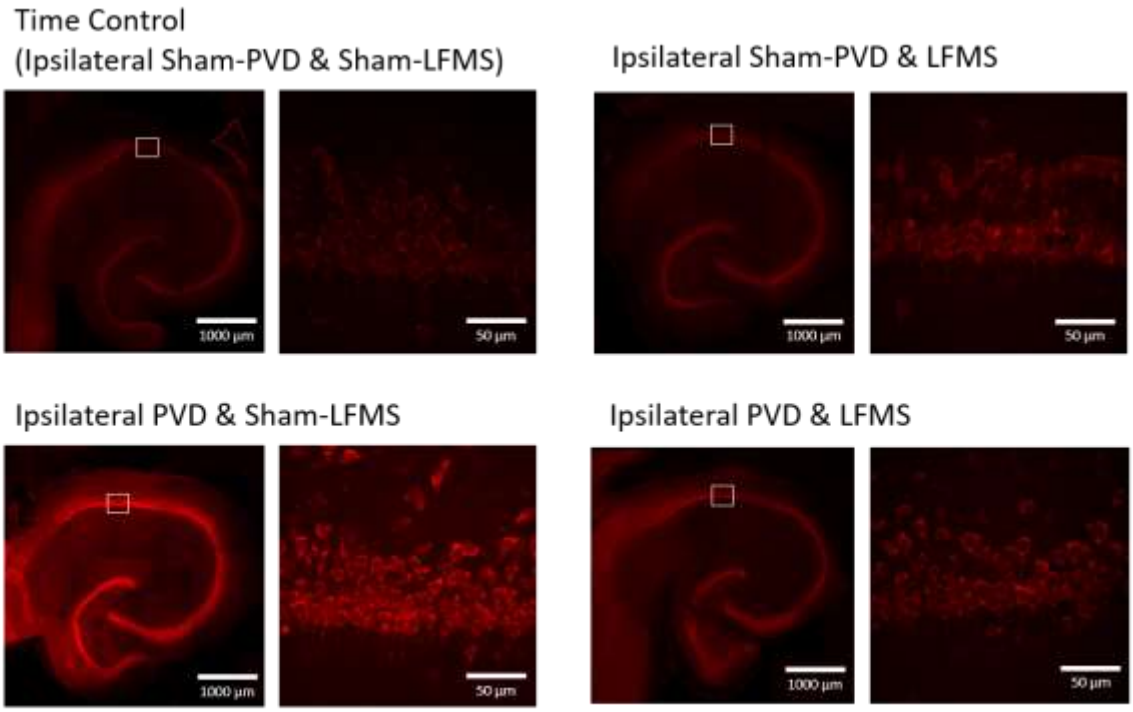
Time Control
(Ipsilateral Sham-PVD & Sham-LFMS)
Ipsilateral Sham-PVD & LFMS
Ipsilateral PVD & Sham-LFMS
Ipsilateral PVD & LFMS
1000 µm
50 µm

b

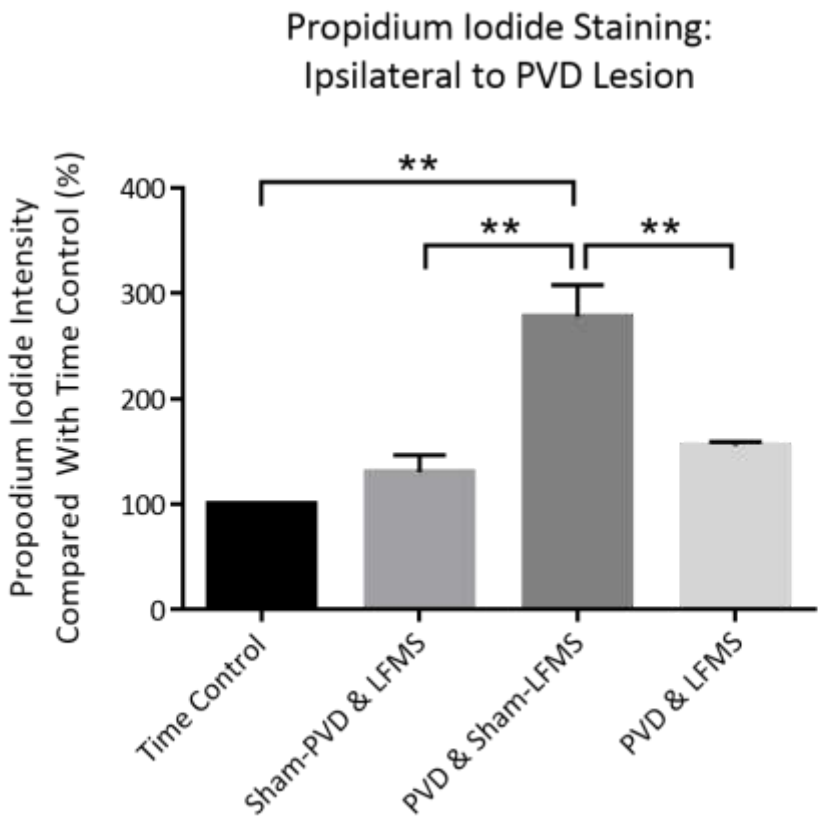
Propidium Iodide Staining:
Ipsilateral to PVD Lesion
Propodium Iodide Intensity
Compared With Time Control (%)
400
300
200
100
0
**
**
**
Time Control
Sham-PVD & LFMS
PVD & Sham-LFMS
PVD & LFMS

c

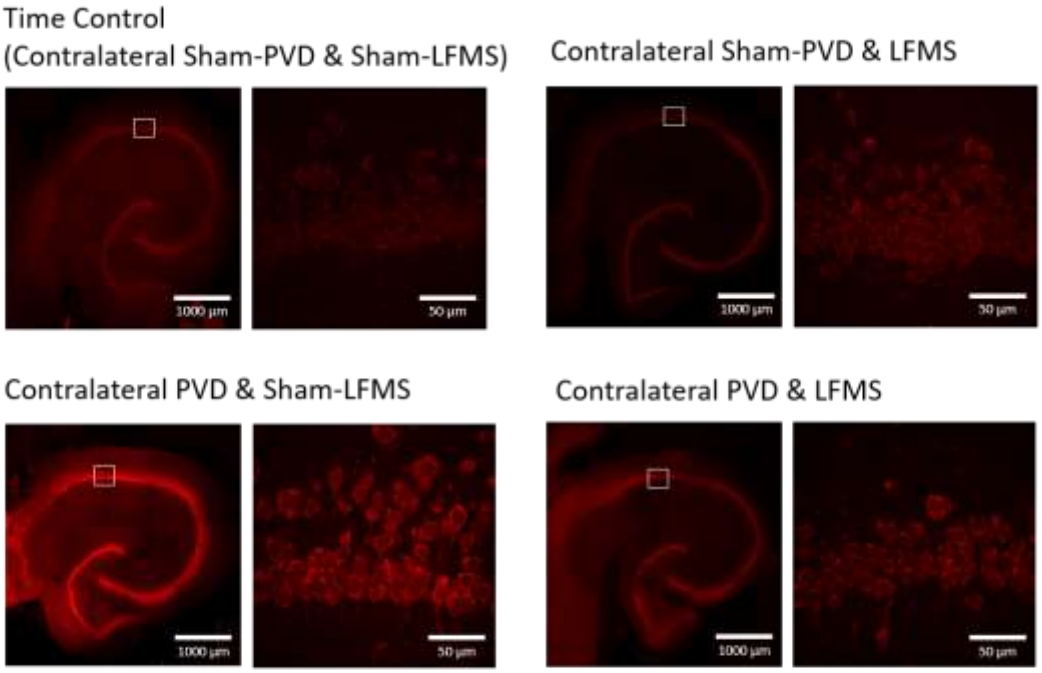
Time Control
(Contralateral Sham-PVD & Sham-LFMS)
Contralateral Sham-PVD & LFMS
Contralateral PVD & Sham-LFMS
Contralateral PVD & LFMS
1000 µm
50 µm

d

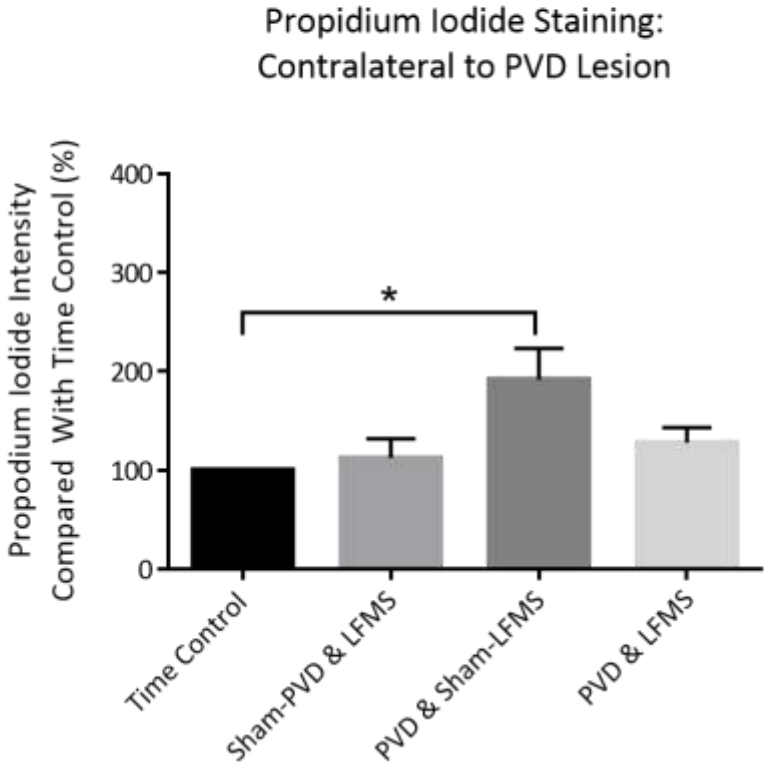
Propidium Iodide Staining:
Contralateral to PVD Lesion
Propodium Iodide Intensity
Compared With Time Control (%)
400
300
200
100
0
*
Time Control
Sham-PVD & LFMS
PVD & Sham-LFMS
PVD & LFMS

Figure 3.6 LFMS treatment reduced cell death in both the ipsilateral and contralateral sides of the PVD lesion. (a-d) Fresh hippocampal slices were stained with PI then imaged with 10x and 63x objective lenses. (a, c) The right panel contains montages of the whole hippocampus, while the left panel contains combined Z-stack images of the CA1. (b, d) Bar graphs showing mean densitometry values normalized to the time control value (100%). (a, b) Amongst the ipsilateral treatment groups, the PVD & Sham-LFMS group fluoresced the brightest indicating the most cell death. LFMS treatment significantly reduced cell death in the ipsilateral hippocampus. (c, d) The contralateral PVD & Sham-LFMS group displayed more cell death compared to the contralateral Sham-PVD & Sham-LFMS group. LFMS did not significantly reduce cell death in the contralateral hippocampus. n=3 independent experiments using four rats per experiment. Values are shown as mean + SEM. Significance values: *= $p<0.05$, **= $p<0.01$.

3.4 LFMS on hippocampal neurodegeneration

While PI confirmed that LFMS rescues hippocampal cells, FJC was specified whether these rescued cells were neurons. Hippocampal LTP is partly dependent on adenosine and glutamate signalling, the disturbance of which (by PVD) causes downstream neurodegeneration (Z. Chen et al., 2014; Lin & Koleske, 2010). Applying gamma oscillations have been found to affect neurons by restoring hippocampal LTP (Komaki, Khalili, Salehi, Shahidi, & Sarihi, 2014; Zhen et al., 2017). Whether this restoration prevents PVD-induced neurodegeneration remains unknown. In the current study, hippocampal slices were washed then stained with FJC for 20 minutes. A Zeiss LSM700 laser scanning confocal microscope was used to image the stained slices. GBOs or LFMS was hypothesized to decrease hippocampal neurodegeneration following PVD.

The PVD & Sham-LFMS group displayed the largest percentage of hippocampal neurodegeneration compared to all other groups (Figure 3.7c, e). LFMS significantly prevented or inhibited this neurodegeneration (Figure 3.7d, e). In fact, the PVD & LFMS group was not significantly different compared to the two Sham-PVD groups, indicating close to full prevention of neurodegeneration by LFMS (Figure 3.7a, b, d, e). Unlike in the PI experiments, the ipsilateral and contralateral sides of the PVD lesion were not separated for FJC staining. Therefore, the different mechanisms and degrees of neuroprotection within each hemisphere cannot be distinguished. PVD-induced neurodegeneration is nonetheless very clear (Z. Chen et al., 2014). Again, more research must be done to understand how the synaptic changes that occur following PVD eventually lead to hippocampal neurodegeneration.

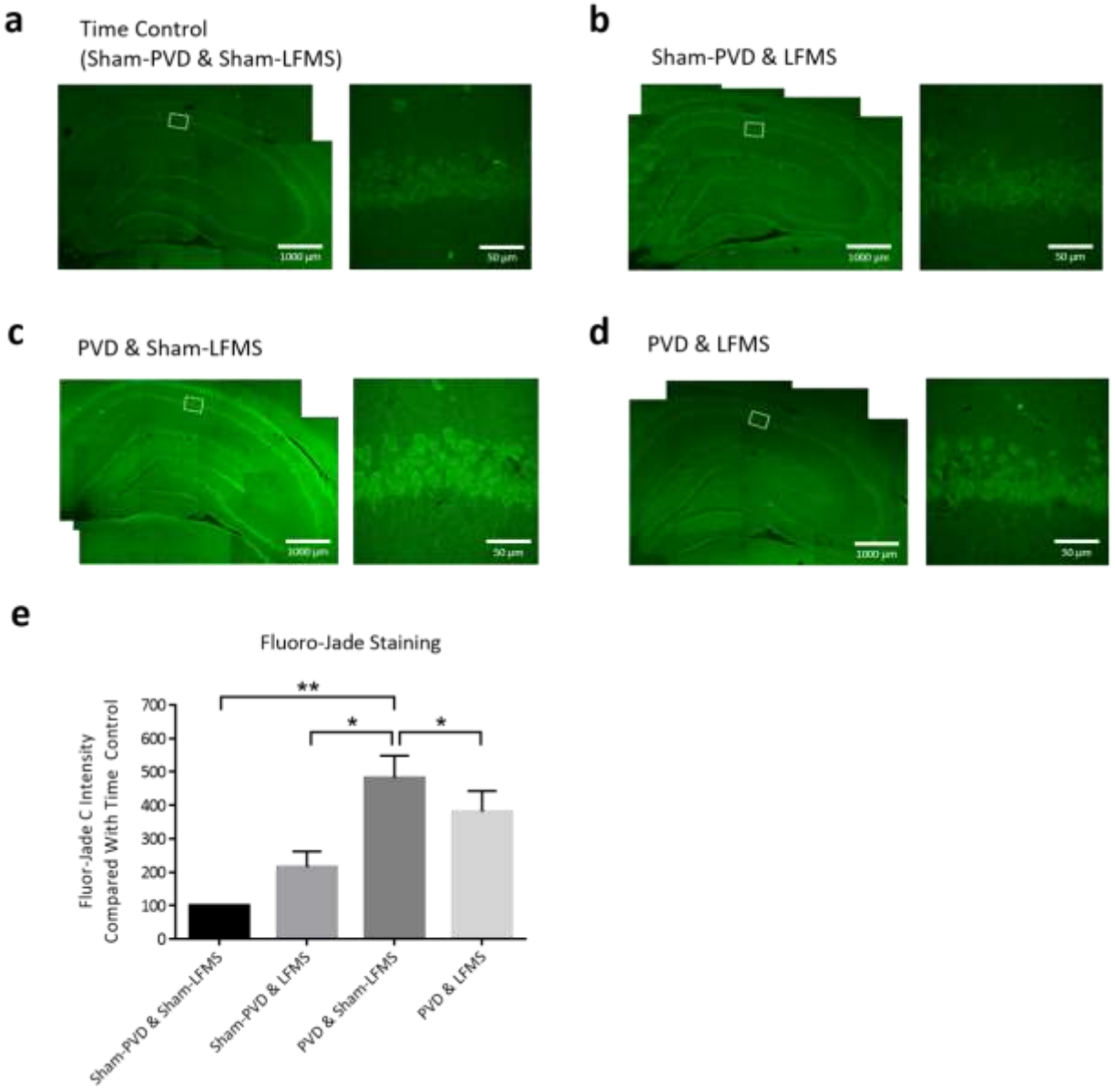

Figure 3.7 LFMS prevents hippocampal neurodegeneration following PVD. (a-e) Fixed hippocampal slices were stained with FJC then imaged with 10x and 63x lenses of a laser scanning confocal microscope. (a-d) The 10x images were combined to form a montage of the whole hippocampus on the left panel. The right panel contains combined Z-stack images of the CA1. (e) Bar graphs showing mean densitometry values normalized to the time control value (100%). (a-e) The PVD & Sham-LFMS group displayed the highest percentage of neurodegeneration compared

to all other groups. This degree of degeneration was significantly reduced in the PVD & LFMS group to the degree where its fluorescence was comparable (not significantly different) to the Sham-PVD groups. The ipsilateral and contralateral hippocampi were not separated in this experiment due to an experimental design error. n=3 independent experiments using four rats per experiment. Values are shown as mean + SEM. Significance values: *= $p<0.05$, **= $p<0.01$.

Chapter 4: Discussion

4.1 LFMS improves emotional and cognitive impairments following PVD.

4.1.1 LFMS alleviates depressive behaviour following PVD.

The FST results indicate that there are strong links between PVD-induced adenosine and glutamate signaling, and depressive behaviour. Rats that underwent PVD and Sham-LFMS displayed the most immobility and the shortest latency to immobility compared to all other treatment groups. PVD causes global increases in extracellular adenosine leading to overstimulation and internalization of A1R; compensatory upregulation of A2AR; and downregulations of GluA1 and GluA2 in the rat hippocampus (Z. Chen et al., 2014). Similarly, A1R knockout mice display depressive behaviour and resistance to the antidepressant effects of sleep deprivation (Serchov et al., 2015), while overexpressing A2AR in the forebrain neurons of rats increases immobility in the FST and decreases sucrose preference at 48 hours in the sucrose preference test (Coelho et al., 2014). Although the literature is clear on how A1R and A2AR differentially regulate depression, it is less clear about non-selective antagonism. For example, caffeine was found to act through A2AR to prevent the mood and memory deficits triggered by chronic stress (Kaster et al., 2015).

GBOs had significant effects on immobility scores in the FST. Compared to the PVD & Sham-LFMS group, rats that underwent PVD and LFMS treatment displayed smaller percentages of time spent immobile and longer latencies to immobility. Not only are hippocampal gamma oscillations disrupted following ischemic stroke, but various studies have reported that gamma oscillation patterns differ between depressed patients and healthy individuals (Akar, Kara, Agambayev, & Bilgic, 2015; Liao, Wu, Huang, Cheng, & Liu, 2017; Pizzagalli, Peccoralo,

Davidson, & Cohen, 2006; Siegle, Condray, Thase, Keshavan, & Steinhauer, 2010; Strelets, Garakh Zh, & Novototskii-Vlasov, 2007). PVD leads to persistent A1R stimulation. Similarly, administering adenosine kinase inhibitor 5-iodotubericidin, A1R agonist PIA, or A2AR antagonist ZM241385 suppressed kainaite-induced gamma oscillation power (Pietersen, Lancaster, Patel, Hamilton, & Vreugdenhil, 2009). Moreover, higher anti-depressant-induced gamma power across brain regions is associated with better response in depressive patients with lower baseline gamma power (Nugent et al., 2018). GBOs may be alleviating depressive behaviour by normalizing adenosine release following PVD, thereby reversing adenosine receptor remodeling, particularly A2AR upregulation.

4.1.2 It remains unclear whether LFMS has an anxiolytic effect in PVD.

Given the high comorbidity of depression and anxiety following a stroke (Schottke & Giabbiconi, 2015), it was hypothesized that the PVD & Sham-LFMS group would also display anxious behaviour in the OFT. However, there were no differences between the groups with regards to center square entries or center square durations. There was a trend where the PVD & Sham-LFMS group entered and stayed in the center square less compared to the other treatment groups. More n-values may be needed for these results to reach significance. According to the literature, the adenosine receptors are regulated differently in anxiety compared to depression. Both CPA and 2-chloro-N6-cyclopentyladenosine, a close analogue of CPA and another selective A1R agonist, were reported as anxiolytic in various behaviour tests (Florio, Prezioso, Papaioannou, & Vertua, 1998; Jain, Kemp, Adeyemo, Buchanan, & Stone, 1995; Prediger, da Silva, Batista, Bittencourt, & Takahashi, 2006). Overexpressing A2AR regardless of A1R in forebrain neurons also leads to anxiolytic effects indicated by hyperlocomotion and increased exploration (Coelho et al., 2014). PVD resembles both of these studies in that persistent A1R

stimulation results in the upregulation of A2AR (M. Chen et al., 2008). The LFMS results may provide a better explanation for PVD causing anxious behaviour in the current study contrary to the literature.

GBOs did not significantly improve anxious behaviour in rats that underwent PVD. The PVD & LFMS group seemed to enter the center square more frequently and stay there for a longer duration compared to the PVD & Sham-LFMS group, however, these differences were not significant. Increased gamma oscillation power is associated with higher anxiety levels (Oathes et al., 2008). For instance, entering an anxious state results in increased gamma power that is prominent in the left temporal regions (Oathes et al., 2008). Moreover, those with generalized anxiety disorder who experience disproportionate worrying tend to exhibit increased gamma oscillation power during worrying compared to undiagnosed subjects (Oathes et al., 2008). Based on the locomotion and center square entries results, rats that received GBOs displayed increased excitability which may be due to an anxiolytic effect. PVD leads to increased adenosine release (Z. Chen et al., 2014), which is linearly related to hippocampal gamma oscillations (Pietersen et al., 2009). LFMS may be exerting its anxiolytic effects through dampening adenosine release following PVD rather than directly modulating the expressions of A1R and A2AR.

4.1.3 LFMS may improve hippocampal-dependent spatial memory following PVD.

Post-stroke hippocampal-dependent spatial memory was measured using novel arm duration in the Y-maze. The PVD & Sham-LFMS group spent significantly less time in the novel arm compared to the control group, represented by the double sham procedure. There was also a trend where the PVD & Sham-LFMS group had a smaller novel arm duration compared to the Sham-PVD & LFMS and PVD & LFMS groups. In one study, A1R knockout mice were reported to have unaffected spatial learning and CA1 synaptic potentiation (Gimenez-Llort et al., 2005).

However, another study showed that A2AR knockout mice had a higher percentage of novel arm visits indicating better hippocampal-dependent spatial memory compared to wild-type CD1 mice (J. H. Wang, Ma, & van den Buuse, 2006). These results indicate that adenosine signaling through A2AR may have a more direct effect on hippocampal-dependent spatial memory compared to A1R activity. PVD does in fact downregulate A2AR leading to glutamatergic changes that impair hippocampal synaptic plasticity (Z. Chen et al., 2014), which underlies processes such as learning and memory.

Although there were no significant differences between the two PVD treatment groups, the PVD & LFMS group's novel arm duration was more similar to the Sham-PVD & Sham-LFMS group compared to the PVD & Sham-LFMS group. These results indicate that LFMS has therapeutic potential in post-stroke hippocampal-dependent spatial memory deficits. Hippocampal gamma oscillations are important for various aspects of working memory. For example, cohesion in gamma oscillations across the hippocampus is present during object-location associative memory encoding (Trimper, Galloway, Jones, Mandi, & Manns, 2017). In another study, theta-gamma oscillation coupling between the hippocampus and the medial prefrontal cortex was augmented during a spatial working memory task, in both cognitively impaired mice and wildtype mice performing in more difficult task settings (Tamura, Spellman, Rosen, Gogos, & Gordon, 2017). Both A2AR agonism and A1R antagonism potentiate kainaite-induced gamma oscillations (Pietersen et al., 2009) in that same way that LFMS aims to increase or resynchronize gamma oscillations to improve cognitive performance following PVD.

4.2 LFMS equalizes hemispheric differences in synaptic plasticity following PVD.

The cLTP experiments assessed aspects of hippocampal synaptic plasticity. As LTP is the neuronal basis for learning and memory, these cLTP results support the findings in the Y-maze.

The contralateral PVD & Sham-LFMS group potentiated the most during cLTP and washout compared to both its ipsilateral counterpart and the Naïve & LFMS group. Thus, different mechanisms of synaptic plasticity are occurring in the ipsilateral and contralateral hippocampus following PVD. One of the best examples of hemispheric differences in plasticity following a stroke can be observed in the motor cortex. Contralateral motor cortex activation is substantially more pronounced compared to the ipsilateral, allowing for the reassignment of lost motor functions after a stroke (Chollet et al., 1991; Pekna, Pekny, & Nilsson, 2012; Zemke, Heagerty, Lee, & Cramer, 2003). Overall, this difference does not compensate well enough to compare to the ability of healthy controls. In the current study, the PVD & Sham-LFMS rats displayed significant impairments in hippocampal-dependent spatial memory compared to the Sham-PVD & Sham-LFMS group

There were no differences between the ipsilateral and contralateral PVD & LFMS groups during either cLTP or washout. However, there was a trend where the ipsilateral group was potentiated more during cLTP. The Naïve & LFMS group also reached higher fEPSPs during cLTP and washout compared to the two PVD & LFMS groups, however, this difference was not significant. These results indicate that GBOs may be equalizing PVD-induced the hemispheric differences. The mechanism of this equalizing effect is unknown. When the network oscillation tracks between the hemispheres are ever disrupted, the right hippocampus assumes a dominant compensatory role in merging the gamma oscillations from each hemisphere and feeding them to neuronal populations with inputs to both (Benito, Martin-Vazquez, Makarova, Makarov, & Herreras, 2016). Thus, GBOs may primarily be working through the right hippocampus in PVD, which may have compromised these tracks.

Overall, the differences in fEPSP during cLTP and washout were not distinguishable by LFMS or Sham-LFMS treatment. Although there was a trend where the ipsilateral and contralateral PVD & Sham-LFMS groups potentiated more during cLTP compared to the two PVD & LFMS groups, this difference was not significant. Both PVD and LFMS have mechanistic links to adenosine signaling and gamma oscillations. As PVD persistent stimulates A1R to disrupt LTP, it may also be suppressing gamma oscillations to impair hippocampal-dependent spatial memory. Moreover, A1R agonism and A2AR antagonism suppresses gamma oscillations, while A1R antagonism and A2AR agonism potentiates gamma oscillations (Pietersen et al., 2009). As previously mentioned, LFMS may be increasing and resynchronizing gamma oscillations following PVD. Pertaining to the cLTP results of the Naïve & LFMS group, the current study does not show differences or advantages in hippocampal spatial memory between the control group and Sham-PVD & LFMS group. However, other studies have shown that TMS delivering frequencies in the 10-20 Hz range enables healthy subjects to continually meet the increasing cognitive demands within a working memory task (Barr et al., 2009; Tamura et al., 2017).

4.3 LFMS employs hemispherically different mechanisms to rescue non-discriminant cells in the hippocampus.

PI staining was conducted to measure non-discriminant cell death in the hippocampus. As hypothesized, the ipsilateral PVD & Sham-LFMS group displayed the most cell death amongst the ipsilateral treatment groups. The contralateral PVD & Sham-PVD group displayed more cell death than only the contralateral Sham-PVD & Sham-PVD. There was no significant difference in cell death between the two contralateral PVD groups. These results support the hemispheric differences in the cLTP data. The synaptic potentiation mechanisms in the ipsilateral hippocampus rescuing more cells compared to the mechanisms occurring in the contralateral hippocampus. In past

experiments when hippocampal slices are exposed to either hypoxia or CPA, both manipulations cause cell death that was reversible by A1R antagonist DPCPX (Stockwell et al., 2016). Thus, GBOs may primarily be targeting persistent A1R stimulation to rescue non-discriminant cells in the hippocampus.

4.4 LFMS reduces hippocampal neurodegeneration.

The hemispheres were not separated prior to FJC staining. Therefore, this data set cannot support the cLTP data showing hemispheric differences in synaptic plasticity. Nonetheless, the PVD & Sham-LFMS group showed significant neurodegeneration, which had been shown in the past (Z. Chen et al., 2014). As it relates to neuroinflammation, the infiltration of peripheral immune cells following an ischemic stroke is thought to exacerbate secondary neurodegeneration. There is greater immune cell infiltration and subsequent neurodegeneration in ipsilateral compared to the contralateral brain regions (Jones et al., 2018). PVD upregulates A2AR, which is also implicated in neuroinflammation. Administering A2AR antagonist SCH58261 attenuates lipopolysaccharide-induced inflammatory mediators and prevents biochemical changes, which otherwise decreased hippocampal LTP (Rebola et al., 2011). Future LFMS studies may delineate the relationships between A1R-modulated neurodegeneration and neuroinflammation in the PVD model.

4.5 Limitations

Acknowledging the limitations of the current study will guide future experiments and further our understanding of how GBOs are therapeutic in post-stroke conditions. The current study only used Sprague Dawley rats that were young adult males. This demographic represents a very small proportion of people who suffer from ischemic stroke. Future studies should also include females and rats of older ages. When it came to the LFMS treatment, it only adopted one

set of stimulation parameters. As previously mentioned, the frequency and temporal pattern, and total time per treatment session may be targeting specific regions and populations of cells more than others. Research on NIBS should focus on adjusting these parameters to target specific aspects of pathophysiology and symptoms. This leads to the experimental design, which measures LFMS-induced behavioral and cellular changes after three days of once-daily LFMS treatments. This is considered short-term and does not imply that these three treatment sessions have sustained therapeutic effects. Future studies should at least continue behaviour testing throughout the month following the PVD and treatments to measure long-term sustainability. Related to behaviour testing, more tests should have been conducted for each psychiatric symptom. For example, the sucrose preference test, Morris water test, and elevated plus maze are additional ways to measure depression, anxiety, and hippocampal-dependent spatial memory, respectively. Related to the treatment groups in the current study, the Naïve & LFMS group was only part of the cLTP experiments. Along with this treatment group, there should also have been a Naïve & Sham-LFMS group to confirm that Sham-PVD surgery has no significant effects on any of the experiments or responding variables. Lastly, the current study lacked groups representing adenosine receptor antagonism. By having a PVD & A1R antagonist (i.e. DPCPX) group and comparing it to the PVD & LFMS group, the therapeutic effects of LFMS could have been attributed to changes in adenosine signaling. This is imperative for future studies, to be able to make correlational links between GBOs or LFMS and adenosine signaling.

4.6 Future Directions

Related to the limitations described in the previous section, the current three-day experimental timeline can be adapted for further pharmacological analysis. By administering an A1R antagonist at the time of the PVD surgery and throughout the rest of the experimental

timeline, persistent A1R stimulation resulting in its desensitization and subsequent adenosine-mediated glutamatergic modulation may be eliminated. Similarly, an A2AR antagonism may prevent the compensatory upregulation in A2AR surface expression and activity. Based on previous studies, antagonizing these receptors is expected to inhibit adenosine-mediated AMPA receptor subunit internalization leading to LTD and impairments in behaviour (Z. Chen et al., 2014; Stockwell et al., 2016). Interestingly, A1R antagonism has been shown to increase the power of endogenous gamma oscillations, while A2AR antagonism is thought to decrease this power (Pietersen et al., 2009). Incorporating either selective or non-selective adenosine antagonism in the current experimental design may better isolate the molecular targets of LFMS in the context of PVD-induced gamma oscillations and intracellular signalling. Aside from receptor activity, PVD-induced extracellular adenosine concentration can also be investigated as a potential therapeutic target. This concentration is measurable via electrophysiological techniques entailing microelectrode biosensors at the level of acute brain slices (Wall, Atterbury, & Dale, 2007). Future studies can also adapt various spatial, temporal, and electromagnetic parameters of the LFMS machine. Different timelines, such as shorter or longer stimulation periods or latencies till behaviour and post-mortem experimentation, may yield valuable pre-clinical information.

The therapeutic potential of LFMS in PVD can be studied in various physiological and anatomical angles. Major stroke-induced pathophysiological processes include excitotoxicity, oxidative stress, neurodegeneration (apoptosis and necrosis), and neuroinflammation (Deb, Sharma, & Hassan, 2010). Occurring concomitantly are repair mechanisms such as neurogenesis, synaptogenesis, oligodendrogenesis, and astroglioses (R. L. Zhang et al., 2012). Future PVD and LFMS experiments can cellularly and molecularly target any of these processes to better understand the therapeutic mechanism of LFMS. Future studies can also investigate different brain

regions implicated in cardiovascular-related emotional and cognitive impairments, as well as regions that are concentrated with A1R and A2AR. Limbic and cortical structures are of particular importance when it comes to depression and anxiety. The frontal-basal ganglia pathway may also be important as it facilitates serotonergic, adrenergic, and dopaminergic neurotransmission (J. S. Kim & Choi-Kwon, 2000). Aside from grey matter, post-PVD white matter may also contain clues about therapeutic mechanism. White matter comprises of axon bundles, myelin and oligodendrocytes. White matter abnormalities in the form of hyperintensities are very common in ischemic stroke and can predict recurrent strokes as well as vascular depression and dementia (Gootjes et al., 2004; Leys et al., 1999). Thus, future studies can also assess whether LFMS is neuroprotective against ischemia through oligodendrogenesis (R. Zhang, Chopp, & Zhang, 2013).

Chapter 5: Conclusion

Based on the findings in the current study, three days of once-daily GBOs following a focal cortical ischemic stroke improved certain aspects of post-stroke emotional and cognitive impairments. Rats that underwent PVD and LFMS displayed less depressive behaviour and restored hippocampal-dependent spatial memory. As for anxiety, there was a trend where LFMS was anxiolytic in rats experiencing PSA. The FST and Y-maze results support the hypothesis that GBOs delivered by LFMS reverses the changes in adenosine signaling caused by PVD. These changes are due to persistent A1R stimulation resulting in its internalization and the subsequent upregulation of A2AR. Based on the literature on adenosine and anxiety, however, increased A1R and decreased A2AR stimulation were expected to be anxiolytic rather than anxiogenic. Thus, LFMS may also have a normalizing effect on any excessive gamma oscillations as a result of PVD, thereby preventing receptor modelling, particularly A1R internalization. When it came to the cLTP experiments, LFMS equalized stroke-induced hemispheric differences in fEPSPs during the induction and washout periods. In other words, GBOs decreased contralateral fEPSPs resulting in the abolishment of its excitotoxic compensatory mechanisms, while improving ipsilateral synaptic plasticity or LTP. Finally, LFMS rescued cells and lessened neurodegeneration in the hippocampus.

References

Aben, I., Lodder, J., Honig, A., Lousberg, R., Boreas, A., & Verhey, F. (2006). Focal or generalized vascular brain damage and vulnerability to depression after stroke: a 1-year prospective follow-up study. *Int Psychogeriatr, 18*(1), 19-35. doi:10.1017/s104161020500270x

Adhikari, A., Topiwala, M. A., & Gordon, J. A. (2010). Synchronized activity between the ventral hippocampus and the medial prefrontal cortex during anxiety. *Neuron, 65*(2), 257-269. doi:10.1016/j.neuron.2009.12.002

Ahmed, O. J., & Mehta, M. R. (2012). Running speed alters the frequency of hippocampal gamma oscillations. *J Neurosci, 32*(21), 7373-7383. doi:10.1523/jneurosci.5110-11.2012

Akar, S. A., Kara, S., Agambayev, S., & Bilgic, V. (2015). Nonlinear analysis of EEG in major depression with fractal dimensions. *Conf Proc IEEE Eng Med Biol Soc, 2015*, 7410-7413. doi:10.1109/embc.2015.7320104

Al-Harbi, K. S., & Qureshi, N. A. (2012). Neuromodulation therapies and treatment-resistant depression. *Medical devices (Auckland, N.Z.), 5*, 53-65. doi:10.2147/MDER.S33198

Albrecht, A., Caliskan, G., Oitzl, M. S., Heinemann, U., & Stork, O. (2013). Long-lasting increase of corticosterone after fear memory reactivation: anxiolytic effects and network activity modulation in the ventral hippocampus. *Neuropsychopharmacology, 38*(3), 386-394. doi:10.1038/npp.2012.192

Bansal, S., Sangha, K. S., & Khatri, P. (2013). Drug treatment of acute ischemic stroke. *Am J Cardiovasc Drugs, 13*(1), 57-69. doi:10.1007/s40256-013-0007-6

Barr, M. S., Farzan, F., Rusjan, P. M., Chen, R., Fitzgerald, P. B., & Daskalakis, Z. J. (2009). Potentiation of gamma oscillatory activity through repetitive transcranial magnetic

stimulation of the dorsolateral prefrontal cortex. *Neuropsychopharmacology, 34*(11), 2359-2367. doi:10.1038/npp.2009.79

Belci, M., Catley, M., Husain, M., Frankel, H. L., & Davey, N. J. (2004). Magnetic brain stimulation can improve clinical outcome in incomplete spinal cord injured patients. *Spinal Cord, 42*(7), 417-419. doi:10.1038/sj.sc.3101613

Benito, N., Martin-Vazquez, G., Makarova, J., Makarov, V. A., & Herreras, O. (2016). The right hippocampus leads the bilateral integration of gamma-parsed lateralized information. *Elife, 5*. doi:10.7554/eLife.16658

Benninger, D. H., Lomarev, M., Lopez, G., Pal, N., Luckenbaugh, D. A., & Hallett, M. (2011). Transcranial direct current stimulation for the treatment of focal hand dystonia. *Mov Disord, 26*(9), 1698-1702. doi:10.1002/mds.23691

Brouns, R., & De Deyn, P. P. (2009). The complexity of neurobiological processes in acute ischemic stroke. *Clin Neurol Neurosurg, 111*(6), 483-495. doi:10.1016/j.clineuro.2009.04.001

Brun, V. H., Otnass, M. K., Molden, S., Steffenach, H. A., Witter, M. P., Moser, M. B., & Moser, E. I. (2002). Place cells and place recognition maintained by direct entorhinal-hippocampal circuitry. *Science, 296*(5576), 2243-2246. doi:10.1126/science.1071089

Brust, T. B., Cayabyab, F. S., & MacVicar, B. A. (2007). C-Jun N-terminal kinase regulates adenosine A1 receptor-mediated synaptic depression in the rat hippocampus. *Neuropharmacology, 53*(8), 906-917. doi:10.1016/j.neuropharm.2007.09.001

Caeiro, L., Ferro, J. M., & Figueira, M. L. (2012). Apathy in acute stroke patients. *Eur J Neurol, 19*(2), 291-297. doi:10.1111/j.1468-1331.2011.03508.x

Caleo, M. (2015). Rehabilitation and plasticity following stroke: Insights from rodent models. *Neuroscience, 311*, 180-194. doi:10.1016/j.neuroscience.2015.10.029

Castillo, C. A., Albasanz, J. L., Leon, D., Jordan, J., Pallas, M., Camins, A., & Martin, M. (2009). Age-related expression of adenosine receptors in brain from the senescence-accelerated mouse. *Exp Gerontol, 44*(6-7), 453-461. doi:10.1016/j.exger.2009.04.006

Cayabyab, F. S., Gowribai, K., & Walz, W. (2013). Involvement of matrix metalloproteinases-2 and -9 in the formation of a lacuna-like cerebral cavity. *J Neurosci Res, 91*(7), 920-933. doi:10.1002/jnr.23223

Chan, S. W., Harmer, C. J., Norbury, R., O'Sullivan, U., Goodwin, G. M., & Portella, M. J. (2016). Hippocampal volume in vulnerability and resilience to depression. *J Affect Disord, 189*, 199-202. doi:10.1016/j.jad.2015.09.021

Chen, M., Lu, T. J., Chen, X. J., Zhou, Y., Chen, Q., Feng, X. Y., . . . Xiong, Z. Q. (2008). Differential roles of NMDA receptor subtypes in ischemic neuronal cell death and ischemic tolerance. *Stroke, 39*(11), 3042-3048. doi:10.1161/strokeaha.108.521898

Chen, Z., Xiong, C., Pancyr, C., Stockwell, J., Walz, W., & Cayabyab, F. S. (2014). Prolonged adenosine A1 receptor activation in hypoxia and pial vessel disruption focal cortical ischemia facilitates clathrin-mediated AMPA receptor endocytosis and long-lasting synaptic inhibition in rat hippocampal CA3-CA1 synapses: differential regulation of GluA2 and GluA1 subunits by p38 MAPK and JNK. *J Neurosci, 34*(29), 9621-9643. doi:10.1523/jneurosci.3991-13.2014

Chollet, F., DiPiero, V., Wise, R. J., Brooks, D. J., Dolan, R. J., & Frackowiak, R. S. (1991). The functional anatomy of motor recovery after stroke in humans: a study with positron emission tomography. *Ann Neurol, 29*(1), 63-71. doi:10.1002/ana.410290112

Chun, H.-Y. Y., Whiteley, W. N., Dennis, M. S., Mead, G. E., & Carson, A. J. (2018). Anxiety After Stroke: The Importance of Subtyping. *Stroke, 49*(3), 556-564. doi:10.1161/STROKEAHA.117.020078

Coelho, J. E., Alves, P., Canas, P. M., Valadas, J. S., Shmidt, T., Batalha, V. L., . . . Lopes, L. V. (2014). Overexpression of Adenosine A2A Receptors in Rats: Effects on Depression, Locomotion, and Anxiety. *Front Psychiatry, 5*, 67. doi:10.3389/fpsyt.2014.00067

Colgin, L. L., Denninger, T., Fyhn, M., Hafting, T., Bonnevie, T., Jensen, O., . . . Moser, E. I. (2009). Frequency of gamma oscillations routes flow of information in the hippocampus. *Nature, 462*(7271), 353-357. doi:10.1038/nature08573

Colgin, L. L., & Moser, E. I. (2010). Gamma oscillations in the hippocampus. *Physiology (Bethesda), 25*(5), 319-329. doi:10.1152/physiol.00021.2010

Collis, M. G., & Hourani, S. M. (1993). Adenosine receptor subtypes. *Trends Pharmacol Sci, 14*(10), 360-366.

Conrad, C. D., Galea, L. A., Kuroda, Y., & McEwen, B. S. (1996). Chronic stress impairs rat spatial memory on the Y maze, and this effect is blocked by tianeptine pretreatment. *Behav Neurosci, 110*(6), 1321-1334.

Costenla, A. R., Cunha, R. A., & de Mendonca, A. (2010). Caffeine, adenosine receptors, and synaptic plasticity. *J Alzheimers Dis, 20 Suppl 1*, S25-34. doi:10.3233/jad-2010-091384

Csicsvari, J., Jamieson, B., Wise, K. D., & Buzsaki, G. (2003). Mechanisms of gamma oscillations in the hippocampus of the behaving rat. *Neuron, 37*(2), 311-322.

Cunha, G. M., Canas, P. M., Oliveira, C. R., & Cunha, R. A. (2006). Increased density and synapto-protective effect of adenosine A2A receptors upon sub-chronic restraint stress. *Neuroscience, 141*(4), 1775-1781. doi:10.1016/j.neuroscience.2006.05.024

de Mendonca, A., & Ribeiro, J. A. (1997). Adenosine and neuronal plasticity. *Life Sci, 60*(4-5), 245-251.

De Renzi, E., Faglioni, P., & Previdi, P. (1977). Spatial memory and hemispheric locus of lesion. *Cortex, 13*(4), 424-433.

Deb, P., Sharma, S., & Hassan, K. M. (2010). Pathophysiologic mechanisms of acute ischemic stroke: An overview with emphasis on therapeutic significance beyond thrombolysis. *Pathophysiology, 17*(3), 197-218. doi:10.1016/j.pathophys.2009.12.001

Di Pino, G., Pellegrino, G., Assenza, G., Capone, F., Ferreri, F., Formica, D., . . . Di Lazzaro, V. (2014). Modulation of brain plasticity in stroke: a novel model for neurorehabilitation. *Nat Rev Neurol, 10*(10), 597-608. doi:10.1038/nrneurol.2014.162

Dilkov, D., Hawken, E. R., Kaludiev, E., & Milev, R. (2017). Repetitive transcranial magnetic stimulation of the right dorsal lateral prefrontal cortex in the treatment of generalized anxiety disorder: A randomized, double-blind sham controlled clinical trial. *Prog Neuropsychopharmacol Biol Psychiatry, 78*, 61-65. doi:10.1016/j.pnpbp.2017.05.018

Dotson, V. M., Szymkowicz, S. M., Kirton, J. W., McLaren, M. E., Green, M. L., & Rohani, J. Y. (2014). Unique and interactive effect of anxiety and depressive symptoms on cognitive and brain function in young and older adults. *J Depress Anxiety, Suppl 1*. doi:10.4172/2167-1044.S1-003

Durukan, A., & Tatlisumak, T. (2007). Acute ischemic stroke: overview of major experimental rodent models, pathophysiology, and therapy of focal cerebral ischemia. *Pharmacol Biochem Behav, 87*(1), 179-197. doi:10.1016/j.pbb.2007.04.015

El Husseini, N., Goldstein, L. B., Peterson, E. D., Zhao, X., Pan, W., Olson, D. M., . . . Laskowitz, D. T. (2012). Depression and antidepressant use after stroke and transient ischemic attack. *Stroke, 43*(6), 1609-1616. doi:10.1161/strokeaha.111.643130

El Yacoubi, M., Ledent, C., Menard, J. F., Parmentier, M., Costentin, J., & Vaugeois, J. M. (2000). The stimulant effects of caffeine on locomotor behaviour in mice are mediated through its blockade of adenosine A(2A) receptors. *Br J Pharmacol, 129*(7), 1465-1473. doi:10.1038/sj.bjp.0703170

Fan, X., Lo, E. H., & Wang, X. (2013). Effects of minocycline plus tissue plasminogen activator combination therapy after focal embolic stroke in type 1 diabetic rats. *Stroke, 44*(3), 745-752. doi:10.1161/STROKEAHA.111.000309

Farach, F. J., Pruitt, L. D., Jun, J. J., Jerud, A. B., Zoellner, L. A., & Roy-Byrne, P. P. (2012). Pharmacological treatment of anxiety disorders: current treatments and future directions. *Journal of anxiety disorders, 26*(8), 833-843. doi:10.1016/j.janxdis.2012.07.009

Feng, C., Fang, M., & Liu, X.-Y. (2014). The neurobiological pathogenesis of poststroke depression. *TheScientificWorldJournal, 2014*, 521349-521349. doi:10.1155/2014/521349

Fitzgerald, P. J., & Watson, B. O. (2018). Gamma oscillations as a biomarker for major depression: an emerging topic. *Transl Psychiatry, 8*(1), 177. doi:10.1038/s41398-018-0239-y

Florio, C., Prezioso, A., Papaioannou, A., & Vertua, R. (1998). Adenosine A1 receptors modulate anxiety in CD1 mice. *Psychopharmacology (Berl), 136*(4), 311-319.

Fredholm, B. B., Chen, J. F., Cunha, R. A., Svenningsson, P., & Vaugeois, J. M. (2005). Adenosine and brain function. *Int Rev Neurobiol, 63,* 191-270. doi:10.1016/s0074-7742(05)63007-3

Freitas, C., Mondragon-Llorca, H., & Pascual-Leone, A. (2011). Noninvasive brain stimulation in Alzheimer's disease: systematic review and perspectives for the future. *Exp Gerontol, 46*(8), 611-627. doi:10.1016/j.exger.2011.04.001

Gimenez-Llort, L., Masino, S. A., Diao, L., Fernandez-Teruel, A., Tobena, A., Halldner, L., & Fredholm, B. B. (2005). Mice lacking the adenosine A1 receptor have normal spatial learning and plasticity in the CA1 region of the hippocampus, but they habituate more slowly. *Synapse, 57*(1), 8-16. doi:10.1002/syn.20146

Gootjes, L., Teipel, S. J., Zebuhr, Y., Schwarz, R., Leinsinger, G., Scheltens, P., . . . Hampel, H. (2004). Regional distribution of white matter hyperintensities in vascular dementia, Alzheimer's disease and healthy aging. *Dement Geriatr Cogn Disord, 18*(2), 180-188. doi:10.1159/000079199

Gottesman, R. F., & Hillis, A. E. (2010). Predictors and assessment of cognitive dysfunction resulting from ischaemic stroke. *Lancet Neurol, 9*(9), 895-905. doi:10.1016/s1474-4422(10)70164-2

Gould, T. J., Rowe, W. B., Heman, K. L., Mesches, M. H., Young, D. A., Rose, G. M., & Bickford, P. C. (2002). Effects of hippocampal lesions on patterned motor learning in the rat. *Brain Res Bull, 58*(6), 581-586.

Grefkes, C., & Ward, N. S. (2014). Cortical reorganization after stroke: how much and how functional? *Neuroscientist, 20*(1), 56-70. doi:10.1177/1073858413491147

Guo, F., Lou, J., Han, X., Deng, Y., & Huang, X. (2017). Repetitive Transcranial Magnetic Stimulation Ameliorates Cognitive Impairment by Enhancing Neurogenesis and Suppressing Apoptosis in the Hippocampus in Rats with Ischemic Stroke. *Front Physiol, 8*, 559. doi:10.3389/fphys.2017.00559

Hafting, T., Fyhn, M., Molden, S., Moser, M. B., & Moser, E. I. (2005). Microstructure of a spatial map in the entorhinal cortex. *Nature, 436*(7052), 801-806. doi:10.1038/nature03721

Harry, G. J., & Lefebvre d'Hellencourt, C. (2003). Dentate gyrus: alterations that occur with hippocampal injury. *Neurotoxicology, 24*(3), 343-356. doi:10.1016/s0161-813x(03)00039-1

Hua, R., & Walz, W. (2006). Minocycline treatment prevents cavitation in rats after a cortical devascularizing lesion. *Brain Res, 1090*(1), 172-181. doi:10.1016/j.brainres.2006.03.072

Iaccarino, H. F., Singer, A. C., Martorell, A. J., Rudenko, A., Gao, F., Gillingham, T. Z., . . . Tsai, L. H. (2018). Author Correction: Gamma frequency entrainment attenuates amyloid load and modifies microglia. *Nature, 562*(7725), E1. doi:10.1038/s41586-018-0351-4

Jain, N., Kemp, N., Adeyemo, O., Buchanan, P., & Stone, T. W. (1995). Anxiolytic activity of adenosine receptor activation in mice. *Br J Pharmacol, 116*(3), 2127-2133.

Johnson, W., Onuma, O., Owolabi, M., & Sachdev, S. (2016). Stroke: a global response is needed. *Bull World Health Organ, 94*(9), 634-634a. doi:10.2471/blt.16.181636

Jones, K. A., Maltby, S., Plank, M. W., Kluge, M., Nilsson, M., Foster, P. S., & Walker, F. R. (2018). Peripheral immune cells infiltrate into sites of secondary neurodegeneration after ischemic stroke. *Brain Behav Immun, 67*, 299-307. doi:10.1016/j.bbi.2017.09.006

Kalaria, R. N., Akinyemi, R., & Ihara, M. (2016). Stroke injury, cognitive impairment and vascular dementia. *Biochim Biophys Acta, 1862*(5), 915-925. doi:10.1016/j.bbadis.2016.01.015

Kaster, M. P., Machado, N. J., Silva, H. B., Nunes, A., Ardais, A. P., Santana, M., . . . Cunha, R. A. (2015). Caffeine acts through neuronal adenosine A2A receptors to prevent mood and memory dysfunction triggered by chronic stress. *Proc Natl Acad Sci U S A, 112*(25), 7833-7838. doi:10.1073/pnas.1423088112

Kazemi, R., Rostami, R., Khomami, S., Horacek, J., Brunovsky, M., Novak, T., & Fitzgerald, P. B. (2016). Electrophysiological correlates of bilateral and unilateral repetitive transcranial magnetic stimulation in patients with bipolar depression. *Psychiatry Res, 240,* 364-375. doi:10.1016/j.psychres.2016.04.061

Khemka, S., Barnes, G., Dolan, R. J., & Bach, D. R. (2017). Dissecting the Function of Hippocampal Oscillations in a Human Anxiety Model. *J Neurosci, 37*(29), 6869-6876. doi:10.1523/jneurosci.1834-16.2017

Kim, B. R., Kim, D. Y., Chun, M. H., Yi, J. H., & Kwon, J. S. (2010). Effect of repetitive transcranial magnetic stimulation on cognition and mood in stroke patients: a double-blind, sham-controlled trial. *Am J Phys Med Rehabil, 89*(5), 362-368. doi:10.1097/PHM.0b013e3181d8a5b1

Kim, J. S., & Choi-Kwon, S. (2000). Poststroke depression and emotional incontinence: correlation with lesion location. *Neurology, 54*(9), 1805-1810.

Komaki, A., Khalili, A., Salehi, I., Shahidi, S., & Sarihi, A. (2014). Effects of exposure to an extremely low frequency electromagnetic field on hippocampal long-term potentiation in rat. *Brain Res, 1564*, 1-8. doi:10.1016/j.brainres.2014.03.041

Kovalenko, T., Osadchenko, I., Nikonenko, A., Lushnikova, I., Voronin, K., Nikonenko, I., . . . Skibo, G. (2006). Ischemia-induced modifications in hippocampal CA1 stratum radiatum excitatory synapses. *Hippocampus, 16*(10), 814-825. doi:10.1002/hipo.20211

Kubis, N. (2016). Non-Invasive Brain Stimulation to Enhance Post-Stroke Recovery. *Front Neural Circuits, 10,* 56. doi:10.3389/fncir.2016.00056

Ledergerber, D., & Larkum, M. E. (2010). Properties of layer 6 pyramidal neuron apical dendrites. *J Neurosci, 30*(39), 13031-13044. doi:10.1523/jneurosci.2254-10.2010

Lee, K., Li, B., Xi, X., Suh, Y., & Martin, R. J. (2005). Role of neuronal energy status in the regulation of adenosine 5'-monophosphate-activated protein kinase, orexigenic neuropeptides expression, and feeding behavior. *Endocrinology, 146*(1), 3-10. doi:10.1210/en.2004-0968

Lenzi, G. L., Altieri, M., & Maestrini, I. (2008). Post-stroke depression. *Rev Neurol (Paris), 164*(10), 837-840. doi:10.1016/j.neurol.2008.07.010

Leys, D., Englund, E., Del Ser, T., Inzitari, D., Fazekas, F., Bornstein, N., . . . Bogousslavsky, J. (1999). White matter changes in stroke patients. Relationship with stroke subtype and outcome. *Eur Neurol, 42*(2), 67-75. doi:10.1159/000069414

Li, W., Huang, R., Shetty, R. A., Thangthaeng, N., Liu, R., Chen, Z., . . . Yang, S. H. (2013). Transient focal cerebral ischemia induces long-term cognitive function deficit in an experimental ischemic stroke model. *Neurobiol Dis, 59*, 18-25. doi:10.1016/j.nbd.2013.06.014

Liao, S. C., Wu, C. T., Huang, H. C., Cheng, W. T., & Liu, Y. H. (2017). Major Depression Detection from EEG Signals Using Kernel Eigen-Filter-Bank Common Spatial Patterns. *Sensors (Basel), 17*(6). doi:10.3390/s17061385

Lin, Y. C., & Koleske, A. J. (2010). Mechanisms of synapse and dendrite maintenance and their disruption in psychiatric and neurodegenerative disorders. *Annu Rev Neurosci, 33*, 349-378. doi:10.1146/annurev-neuro-060909-153204

Lu, B., Nagappan, G., & Lu, Y. (2014). BDNF and Synaptic Plasticity, Cognitive Function, and Dysfunction. In G. R. Lewin & B. D. Carter (Eds.), *Neurotrophic Factors* (pp. 223-250). Berlin, Heidelberg: Springer Berlin Heidelberg.

Luber, B., & Lisanby, S. H. (2014). Enhancement of human cognitive performance using transcranial magnetic stimulation (TMS). *Neuroimage, 85 Pt 3*, 961-970. doi:10.1016/j.neuroimage.2013.06.007

Mably, A. J., & Colgin, L. L. (2018). Gamma oscillations in cognitive disorders. *Curr Opin Neurobiol, 52*, 182-187. doi:10.1016/j.conb.2018.07.009

Madinier, A., Bertrand, N., Rodier, M., Quirie, A., Mossiat, C., Prigent-Tessier, A., . . . Garnier, P. (2013). Ipsilateral versus contralateral spontaneous post-stroke neuroplastic changes: involvement of BDNF? *Neuroscience, 231*, 169-181. doi:10.1016/j.neuroscience.2012.11.054

Marshall, R. S., Perera, G. M., Lazar, R. M., Krakauer, J. W., Constantine, R. C., & DeLaPaz, R. L. (2000). Evolution of cortical activation during recovery from corticospinal tract infarction. *Stroke, 31*(3), 656-661.

Martin, E. I., Ressler, K. J., Binder, E., & Nemeroff, C. B. (2009). The neurobiology of anxiety disorders: brain imaging, genetics, and psychoneuroendocrinology. *Psychiatr Clin North Am, 32*(3), 549-575. doi:10.1016/j.psc.2009.05.004

Martin, E. I., Ressler, K. J., Binder, E., & Nemeroff, C. B. (2009). The neurobiology of anxiety disorders: brain imaging, genetics, and psychoneuroendocrinology. *The Psychiatric clinics of North America, 32*(3), 549-575. doi:10.1016/j.psc.2009.05.004

Modrego, P. J. (2010). Depression in Alzheimer's disease. Pathophysiology, diagnosis, and treatment. *J Alzheimers Dis, 21*(4), 1077-1087.

Moyanova, S. G., & Dijkhuizen, R. M. (2014). Present status and future challenges of electroencephalography- and magnetic resonance imaging-based monitoring in preclinical

models of focal cerebral ischemia. *Brain Res Bull, 102*, 22-36. doi:10.1016/j.brainresbull.2014.01.003

NIH. (2018). Post-Stroke Rehabilitation Fact Sheet, https://www.ninds.nih.gov/Disorders/Patient-Caregiver-Education/Fact-Sheets/Post-Stroke-Rehabilitation-Fact-Sheet.

Nishizawa, Y. (2001). Glutamate release and neuronal damage in ischemia. *Life Sci, 69*(4), 369-381.

Nugent, A. C., Ballard, E. D., Gould, T. D., Park, L. T., Moaddel, R., Brutsche, N. E., & Zarate, C. A., Jr. (2018). Ketamine has distinct electrophysiological and behavioral effects in depressed and healthy subjects. *Mol Psychiatry*. doi:10.1038/s41380-018-0028-2

Oathes, D. J., Ray, W. J., Yamasaki, A. S., Borkovec, T. D., Castonguay, L. G., Newman, M. G., & Nitschke, J. (2008). Worry, generalized anxiety disorder, and emotion: evidence from the EEG gamma band. *Biol Psychol, 79*(2), 165-170. doi:10.1016/j.biopsycho.2008.04.005

Padilla-Coreano, N., Bolkan, S. S., Pierce, G. M., Blackman, D. R., Hardin, W. D., Garcia-Garcia, A. L., . . . Gordon, J. A. (2016). Direct Ventral Hippocampal-Prefrontal Input Is Required for Anxiety-Related Neural Activity and Behavior. *Neuron, 89*(4), 857-866. doi:10.1016/j.neuron.2016.01.011

Paolucci, S. (2008). Epidemiology and treatment of post-stroke depression. *Neuropsychiatr Dis Treat, 4*(1), 145-154.

Pekna, M., Pekny, M., & Nilsson, M. (2012). Modulation of neural plasticity as a basis for stroke rehabilitation. *Stroke, 43*(10), 2819-2828. doi:10.1161/strokeaha.112.654228

Pietersen, A. N., Lancaster, D. M., Patel, N., Hamilton, J. B., & Vreugdenhil, M. (2009). Modulation of gamma oscillations by endogenous adenosine through A1 and A2A

receptors in the mouse hippocampus. *Neuropharmacology, 56*(2), 481-492. doi:10.1016/j.neuropharm.2008.10.001

Pizzagalli, D. A., Peccoralo, L. A., Davidson, R. J., & Cohen, J. D. (2006). Resting anterior cingulate activity and abnormal responses to errors in subjects with elevated depressive symptoms: a 128-channel EEG study. *Hum Brain Mapp, 27*(3), 185-201. doi:10.1002/hbm.20172

Prediger, R. D., da Silva, G. E., Batista, L. C., Bittencourt, A. L., & Takahashi, R. N. (2006). Activation of adenosine A1 receptors reduces anxiety-like behavior during acute ethanol withdrawal (hangover) in mice. *Neuropsychopharmacology, 31*(10), 2210-2220. doi:10.1038/sj.npp.1301001

Radak, D., Resanovic, I., & Isenovic, E. R. (2014). Changes in hypothalamus-pituitary-adrenal axis following transient ischemic attack. *Angiology, 65*(8), 723-732. doi:10.1177/0003319713503487

Rebholz, H., Nishi, A., Liebscher, S., Nairn, A. C., Flajolet, M., & Greengard, P. (2009). CK2 negatively regulates Galphas signaling. *Proc Natl Acad Sci U S A, 106*(33), 14096-14101. doi:10.1073/pnas.0906857106

Rebola, N., Simoes, A. P., Canas, P. M., Tome, A. R., Andrade, G. M., Barry, C. E., . . . Cunha, R. A. (2011). Adenosine A2A receptors control neuroinflammation and consequent hippocampal neuronal dysfunction. *J Neurochem, 117*(1), 100-111. doi:10.1111/j.1471-4159.2011.07178.x

Rist, P. M., Chalmers, J., Arima, H., Anderson, C., Macmahon, S., Woodward, M., . . . Tzourio, C. (2013). Baseline cognitive function, recurrent stroke, and risk of dementia in patients with stroke. *Stroke, 44*(7), 1790-1795. doi:10.1161/strokeaha.111.680728

Rohan, M. (2015). http://lfms.mclean.harvard.edu/clinical-studies.

Rohan, M., Parow, A., Stoll, A. L., Demopulos, C., Friedman, S., Dager, S., . . . Renshaw, P. F. (2004). Low-field magnetic stimulation in bipolar depression using an MRI-based stimulator. *Am J Psychiatry, 161*(1), 93-98. doi:10.1176/appi.ajp.161.1.93

Rohan, M. L., Yamamoto, R. T., Ravichandran, C. T., Cayetano, K. R., Morales, O. G., Olson, D. P., . . . Cohen, B. M. (2014). Rapid mood-elevating effects of low field magnetic stimulation in depression. *Biol Psychiatry, 76*(3), 186-193. doi:10.1016/j.biopsych.2013.10.024

Rudolphi, K. A., Schubert, P., Parkinson, F. E., & Fredholm, B. B. (1992). Adenosine and brain ischemia. *Cerebrovasc Brain Metab Rev, 4*(4), 346-369.

Sasaki, N., Hara, T., Yamada, N., Niimi, M., Kakuda, W., & Abo, M. (2017). The Efficacy of High-Frequency Repetitive Transcranial Magnetic Stimulation for Improving Apathy in Chronic Stroke Patients. *Eur Neurol, 78*(1-2), 28-32. doi:10.1159/000477440

Schmidt-Kastner, R., & Freund, T. F. (1991). Selective vulnerability of the hippocampus in brain ischemia. *Neuroscience, 40*(3), 599-636.

Schneider, T. R., Hipp, J. F., Domnick, C., Carl, C., Buchel, C., & Engel, A. K. (2018). Modulation of neuronal oscillatory activity in the beta- and gamma-band is associated with current individual anxiety levels. *Neuroimage, 178*, 423-434. doi:10.1016/j.neuroimage.2018.05.059

Schottke, H., & Giabbiconi, C. M. (2015). Post-stroke depression and post-stroke anxiety: prevalence and predictors. *Int Psychogeriatr, 27*(11), 1805-1812. doi:10.1017/s1041610215000988

Sebastião, A. M., de Mendonça, A., & Ribeiro, J. A. (2001). Neuroprotection during hypoxic insults: Role of adenosine. *Drug Development Research, 52*(1-2), 291-295. doi:10.1002/ddr.1126

Serchov, T., Clement, H. W., Schwarz, M. K., Iasevoli, F., Tosh, D. K., Idzko, M., . . . van Calker, D. (2015). Increased Signaling via Adenosine A1 Receptors, Sleep Deprivation, Imipramine, and Ketamine Inhibit Depressive-like Behavior via Induction of Homer1a. *Neuron, 87*(3), 549-562. doi:10.1016/j.neuron.2015.07.010

Shafi, M., Stern, A. P., & Pascual-Leone, A. (2014). Adding low-field magnetic stimulation to noninvasive electromagnetic neuromodulatory therapies. *Biol Psychiatry, 76*(3), 170-171. doi:10.1016/j.biopsych.2014.05.017

Siegle, G. J., Condray, R., Thase, M. E., Keshavan, M., & Steinhauer, S. R. (2010). Sustained gamma-band EEG following negative words in depression and schizophrenia. *International journal of psychophysiology : official journal of the International Organization of Psychophysiology, 75*(2), 107-118. doi:10.1016/j.ijpsycho.2008.04.008

Snaphaan, L., van der Werf, S., Kanselaar, K., & de Leeuw, F. E. (2009). Post-stroke depressive symptoms are associated with post-stroke characteristics. *Cerebrovasc Dis, 28*(6), 551-557. doi:10.1159/000247598

Spruston, N. (2008). Pyramidal neurons: dendritic structure and synaptic integration. *Nat Rev Neurosci, 9*(3), 206-221. doi:10.1038/nrn2286

Steffenach, H. A., Sloviter, R. S., Moser, E. I., & Moser, M. B. (2002). Impaired retention of spatial memory after transection of longitudinally oriented axons of hippocampal CA3 pyramidal cells. *Proc Natl Acad Sci U S A, 99*(5), 3194-3198. doi:10.1073/pnas.042700999

Stockwell, J., Chen, Z., Niazi, M., Nosib, S., & Cayabyab, F. S. (2016). Protein phosphatase role in adenosine A1 receptor-induced AMPA receptor trafficking and rat hippocampal neuronal damage in hypoxia/reperfusion injury. *Neuropharmacology, 102*, 254-265. doi:10.1016/j.neuropharm.2015.11.018

Stockwell, J., Jakova, E., & Cayabyab, F. S. (2017). Adenosine A1 and A2A Receptors in the Brain: Current Research and Their Role in Neurodegeneration. *Molecules, 22*(4). doi:10.3390/molecules22040676

Strelets, V. B., Garakh Zh, V., & Novototskii-Vlasov, V. Y. (2007). Comparative study of the gamma rhythm in normal conditions, during examination stress, and in patients with first depressive episode. *Neurosci Behav Physiol, 37*(4), 387-394. doi:10.1007/s11055-007-0025-4

Tamura, M., Spellman, T. J., Rosen, A. M., Gogos, J. A., & Gordon, J. A. (2017). Hippocampal-prefrontal theta-gamma coupling during performance of a spatial working memory task. *Nature communications, 8*(1), 2182-2182. doi:10.1038/s41467-017-02108-9

Tatu, L., & Vuillier, F. (2014). Structure and vascularization of the human hippocampus. *Front Neurol Neurosci, 34*, 18-25. doi:10.1159/000356440

Tranchina, D., & Nicholson, C. (1986). A model for the polarization of neurons by extrinsically applied electric fields. *Biophysical journal, 50*(6), 1139-1156. doi:10.1016/S0006-3495(86)83558-5

Trimper, J. B., Galloway, C. R., Jones, A. C., Mandi, K., & Manns, J. R. (2017). Gamma Oscillations in Rat Hippocampal Subregions Dentate Gyrus, CA3, CA1, and Subiculum Underlie Associative Memory Encoding. *Cell Rep, 21*(9), 2419-2432. doi:10.1016/j.celrep.2017.10.123

Tyler, W. J., Tufail, Y., Finsterwald, M., Tauchmann, M. L., Olson, E. J., & Majestic, C. (2008). Remote excitation of neuronal circuits using low-intensity, low-frequency ultrasound. *PLoS One, 3*(10), e3511. doi:10.1371/journal.pone.0003511

Van Kanegan, M. J., He, D. N., Dunn, D. E., Yang, P., Newman, R. A., West, A. E., & Lo, D. C. (2014). BDNF mediates neuroprotection against oxygen-glucose deprivation by the cardiac glycoside oleandrin. *The Journal of neuroscience : the official journal of the Society for Neuroscience, 34*(3), 963-968. doi:10.1523/JNEUROSCI.2700-13.2014

Volpe, B. T., Davis, H. P., Towle, A., & Dunlap, W. P. (1992). Loss of hippocampal CA1 pyramidal neurons correlates with memory impairment in rats with ischemic or neurotoxin lesions. *Behav Neurosci, 106*(3), 457-464.

Wall, M. J., Atterbury, A., & Dale, N. (2007). Control of basal extracellular adenosine concentration in rat cerebellum. *J Physiol, 582*(Pt 1), 137-151. doi:10.1113/jphysiol.2007.132050

Wang, J. H., Ma, Y. Y., & van den Buuse, M. (2006). Improved spatial recognition memory in mice lacking adenosine A2A receptors. *Exp Neurol, 199*(2), 438-445. doi:10.1016/j.expneurol.2006.01.005

Wang, K., & Walz, W. (2003). Unusual topographical pattern of proximal astrogliosis around a cortical devascularizing lesion. *J Neurosci Res, 73*(4), 497-506. doi:10.1002/jnr.10683

Ward, N. S., Brown, M. M., Thompson, A. J., & Frackowiak, R. S. (2003). Neural correlates of motor recovery after stroke: a longitudinal fMRI study. *Brain, 126*(Pt 11), 2476-2496. doi:10.1093/brain/awg245

Webster, B. R., Celnik, P. A., & Cohen, L. G. (2006). Noninvasive brain stimulation in stroke rehabilitation. *NeuroRx, 3*(4), 474-481. doi:10.1016/j.nurx.2006.07.008

Wei, J., Fang, W., Sha, L., Han, D., Zhang, R., Hao, X., & Li, Y. (2013). XQ-1H Suppresses Neutrophils Infiltration and Oxidative Stress Induced by Cerebral Ischemia Injury Both In Vivo and In Vitro. *Neurochem Res*. doi:10.1007/s11064-013-1176-z

Wright, F., Wu, S., Chun, H. Y., & Mead, G. (2017). Factors Associated with Poststroke Anxiety: A Systematic Review and Meta-Analysis. *Stroke Res Treat, 2017*, 2124743. doi:10.1155/2017/2124743

Xiao, L., Correll, C. U., Feng, L., Xiang, Y. T., Feng, Y., Hu, C. Q., . . . Wang, G. (2018). Rhythmic low-field magnetic stimulation may improve depression by increasing brain-derived neurotrophic factor. *CNS Spectr*, 1-9. doi:10.1017/s1092852917000670

Yabuki, Y., & Fukunaga, K. (2013). Oral administration of glutathione improves memory deficits following transient brain ischemia by reducing brain oxidative stress. *Neuroscience, 250*, 394-407. doi:10.1016/j.neuroscience.2013.07.017

Yamamoto, J., Suh, J., Takeuchi, D., & Tonegawa, S. (2014). Successful execution of working memory linked to synchronized high-frequency gamma oscillations. *Cell, 157*(4), 845-857. doi:10.1016/j.cell.2014.04.009

Yang, J., Yao, Y., Chen, T., & Zhang, T. (2014). VEGF ameliorates cognitive impairment in in vivo and in vitro ischemia via improving neuronal viability and function. *Neuromolecular Med, 16*(2), 376-388. doi:10.1007/s12017-013-8284-4

Yankelevitch-Yahav, R., Franko, M., Huly, A., & Doron, R. (2015). The forced swim test as a model of depressive-like behavior. *J Vis Exp*(97). doi:10.3791/52587

Zemke, A. C., Heagerty, P. J., Lee, C., & Cramer, S. C. (2003). Motor cortex organization after stroke is related to side of stroke and level of recovery. *Stroke, 34*(5), e23-28. doi:10.1161/01.Str.0000065827.35634.5e

Zhang, R., Chopp, M., & Zhang, Z. G. (2013). Oligodendrogenesis after cerebral ischemia. *Front Cell Neurosci, 7*, 201. doi:10.3389/fncel.2013.00201

Zhang, R. L., Chopp, M., Roberts, C., Wei, M., Wang, X., Liu, X., . . . Zhang, Z. G. (2012). Sildenafil enhances neurogenesis and oligodendrogenesis in ischemic brain of middle-aged mouse. *PLoS One, 7*(10), e48141. doi:10.1371/journal.pone.0048141

Zhen, J., Qian, Y., Weng, X., Su, W., Zhang, J., Cai, L., . . . Wang, X. (2017). Gamma rhythm low field magnetic stimulation alleviates neuropathologic changes and rescues memory and cognitive impairments in a mouse model of Alzheimer's disease. *Alzheimers Dement (N Y), 3*(4), 487-497. doi:10.1016/j.trci.2017.07.002

Zhu, H., Yoshimoto, T., Imajo-Ohmi, S., Dazortsava, M., Mathivanan, A., & Yamashima, T. (2012). Why are hippocampal CA1 neurons vulnerable but motor cortex neurons resistant to transient ischemia? *J Neurochem, 120*(4), 574-585. doi:10.1111/j.1471-4159.2011.07550.x